Innoslab Amplifiers

Peter Russbueldt, Dieter Hoffmann, Marco Höfer, Jens Löhring, Jörg Luttmann, Ansgar Meissner, Johannes Weitenberg, Martin Traub, Thomas Sartorius, Dominik Esser, Rolf Wester, Peter Loosen, and Reinhart Poprawe

(Invited Paper)

***Abstract*—The Innoslab amplifier comprises a diode-laser partially end-pumped thin slab crystal and a folded single-pass optical amplification path. While this configuration differs in many respects from other slab amplifiers, it shares characteristics with partially end-pumped rod amplifiers. It combines outstanding thermal management, efficiency, and beam quality in the 100 W to 1 kW power range. In this paper, we review amplifiers for a wide range of operation regimes and laser materials.**

***Index Terms*—Optical amplifiers, power lasers, solid lasers.**

I. Introduction

INNOSLAB is a laser design based on slab shaped laser crystals, which was developed and patented in 1996 by K. Du at the Fraunhofer Institute for Laser Technology, Aachen, Germany [1], [2]. The name Innoslab was chosen to distinguish the new concept from earlier or other slab designs. The Innoslab is defined by a longitudinal pumping of the gain volume in the crystal in combination with an appropriate beam path. The setup will be described in more detail in Section II.

The Innoslab development started in 1994 when a laser crystal was longitudinally pumped with a collimated diode laser bar. A stable resonator configuration provided a high aspect ratio, elliptical beam profile with a high beam quality in the small transverse dimension and a high order mode in the large transverse dimension. A very high efficiency comparable to end-pumped rod lasers was observed. In the following years an oscillator design with a hybrid resonator was investigated in order to achieve high beam quality at high efficiency in both transverse directions of the beam. Significant effort was put into improvement of the conduction cooling of the slab and the beam shaping and homogenization of the pump radiation.

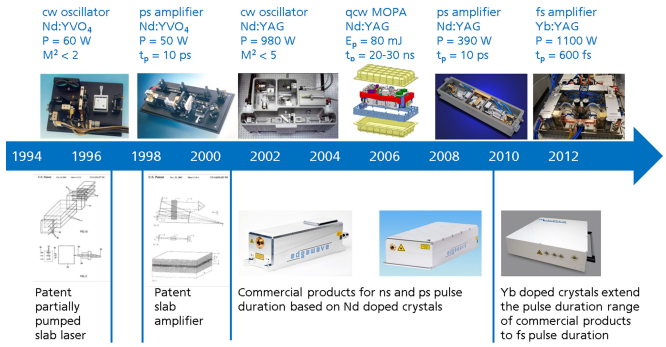

Fig. 1. Major development steps of Innoslab lasers and amplifiers.

The Innoslab amplifier configuration was developed in 1998 and a very encouraging output power of more than 50 W at 13 ps pulse duration could be demonstrated with an amplifier shipped to the Australian National University. Fig. 1 provides a short overview of the major development steps including the foundation of spin-off companies with the Innoslab as their core product. Important achievements were the demonstration of about 1 kW continuous wave (cw) output power out of a single crystal oscillator in 2002 [3] and the demonstration of a bandwidth-limited MOPA for LIDAR applications providing 80 mJ pulse energy at about 30 ns pulse duration at very high efficiency [4]. Since ultrafast pulses became important for industrial applications, the demonstration of 400 W output power at 11 ps pulse duration with Nd-doped crystals [41] and 1.1 kW output power at about 600 fs pulse duration with Yb-doped crystals [54] pave the way for high precision, high throughput processing with ultrashort pulses for industrial processes.

The following section provides a brief history and overview of earlier or other designs of slab-based amplifier modules. In this text the following definition of "slab laser" is used: a slab laser has at least one transverse dimension of the gain medium, which is significantly smaller than the longitudinal beam path inside the gain medium. At least four crystal surfaces have a rectangular shape. By this definition slab lasers/amplifiers can be distinguished from other configurations, such as disk lasers/amplifiers.

Historically slab lasers have been "face pumped" by lamps through the large surfaces leading to pump absorption more or less in the entire crystal volume. The large surfaces are also used for cooling by transparent fluids or gases, thus providing one-dimensional heat flow. As a third function, the large faces reflect

Manuscript received April 1, 2014; revised June 16, 2014; accepted June 17, 2014. Date of publication June 25, 2014; date of current version August 22, 2014. This work was supported by the Federal Ministry of Education and Research and of the Federal Ministry for Economic Affairs and Technology under Contracts 01LK0905B, 50EE1222, 50EE1228, 50EE0516, 50EE0714, 13N8717, 13N8293, and 13N11628.

P. Russbueldt, D. Hoffmann, M. Höfer, J. Löhring, J. Luttmann, A. Meissner, M. Traub, T. Sartorius, D. Esser, and R. Wester are with the Fraunhofer Institute for Laser Technology, D-52074 Aachen, Germany (e-mail: peter.russbueldt@ilt.fraunhofer.de; hansdieter.hoffmann@ilt.fraunhofer.de; marco.hoefer@ilt.fraunhofer.de; jens.loehring@ilt.fraunhofer.de; joerg.luttmann@ilt.fraunhofer.de; ansgar.meissner@ilt.fraunhofer.de; martin.traub@ilt.fraunhofer.de; thomas.sartorius@ilt.fraunhoffer.de; dominik.esser@ilt.fraunhofer.de; rolf.wester@ilt.fraunhofer.de).

J. Weitenberg is with the Chair for Laser Technology, RWTH Aachen University, D-52074 Aachen (e-mail: johannes.weitenberg@ilt.fraunhofer.de).

P. Loosen is with the Chair for Technology of Optical Systems, RWTH Aachen University, D-52074 Aachen (e-mail: peter.loosen@ilt.fraunhofer.de).

R. Poprawe is with the Fraunhofer Institute for Laser Technology, D-52074 Aachen, Germany, and also with the Chair for Laser Technology RWTH Aachen University, D-52074 Aachen, Germany (e-mail: reinhart.poprawe@ilt.fraunhofer.de).

Color versions of one or more of the figures in this paper are available online at http://ieeexplore.ieee.org.

Digital Object Identifier 10.1109/JSTQE.2014.2333234

the laser beam, thereby providing a zigzag beam path between the cooled surfaces which compensates for thermal-lens effects [6], [7]. The two end faces are antireflection coated for the amplified laser beam. In early designs Brewster cut end faces were used to suppress parasitic oscillations. Face-pumped slabs have at least four optical grade polished optically functional surfaces.

In a next development step flash-lamps for pulsed pumping and arc-lamps for continuous pumping were replaced by stacked diode laser arrays. Better absorption of the diode emission allowed for a smaller slab cross section and improved efficiency. The high optical brightness of the diode lasers allows for pumping through the small side faces [5] or end faces [6] of the slab. This makes it possible to use conductive cooling as an option. In these configurations the complete crystal volume is pumped. The slab crystal has four to six optical grade polished functional surfaces. The pump arrangement of these slab lasers is comparably compact, but significant effort has to be spent into suppression of parasitic oscillations caused by the multiple reflective surfaces as well as reduction of thermally induced distortions. Measures taken to prevent these effects include coated edges, undoped sections bonded to the slab or a zigzag beam path for the amplified laser beam. For further beam quality improvement phase conjugating concepts were demonstrated [6]. Taking a look at commercial products based on these "conventional" designs, we see that slab lasers from companies such as CUTTING EDGE OPTRONICS (diode-pumped OEM amplifier module), QUANTEL (QCW diode-pumped amplifier for operation in space) and LASAG (QCW lamp-pumped oscillator for precision cutting applications) have found some niche applications where their performance justified the comparably high costs. An overview of several slab concepts is provided in [7].

In order to achieve a better overlap of gain volume and amplified beam, waveguide-based slab designs have been investigated [8]–[10]. The pump scheme is comparable to core- or cladding-pumped fiber lasers. The high aspect ratio pump apertures match well to the emission characteristics of diode laser arrays. Waveguide-based slab designs have six or even more optical grade functional surfaces or flat interfaces with index steps. Parasitic oscillations at high gain have to be considered carefully.

Further advanced slab designs make use of the capability of high power diode lasers to provide collimated pump light. Only the exploited gain volume is selectively pumped in a side-pump configuration. The transversally pumped multipass slab [11] provides a compact pump scheme and good performance in the multi 10 W power range. Several crystal materials have been demonstrated. The best performance is achieved with YLF crystals, if the crystal axis with weak thermal lensing is oriented in the direction of the propagating pump radiation. Another transversally pumped configuration is the bounce amplifier [12]. This compact design offers very high gain at multi 10 W average power.

All slab configurations except the Innoslab require more than two optically grade polished functional surfaces and have to cope with internal parasitic effects, especially in the pulsed mode, where very high gain occurs at the end of the pump phase.

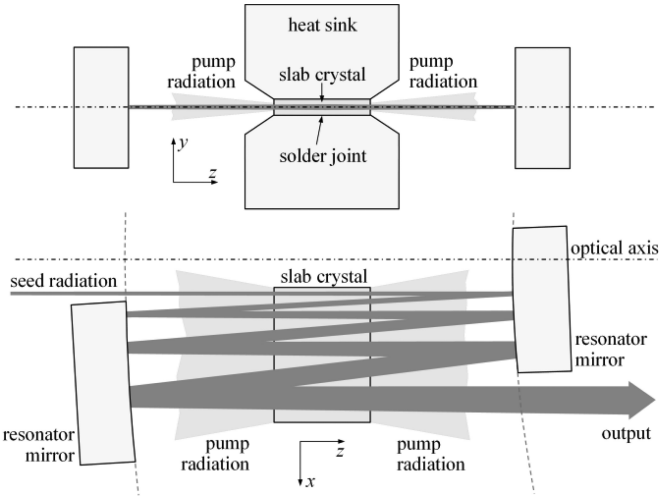

Fig. 2. Resonator setup of an Innoslab amplifier in stable or y-direction (top) and in unstable or x-direction (bottom). The magnification of the confocal arrangement in unstable direction is $M = 1.6$ in the sketch.

In transverse or side-pumping schemes, variations in pump absorption and temperature profiles may lead to degradation of the beam quality or the beam pointing.

As the gain in Innoslab amplifiers can be tailored by varying the shape of the gain volume, the number of beam passes and the cross section of the amplified beam, a large variety of gain media is compatible with the design. In particular results with Nd:YAG [4], [22], Nd:YVO_4 [40]–[44], Yb:YAG [51]–[60], Yb:KYW [13], Tm:YLF [38], Nd:YGG [27] have been published.

The Innoslab amplifier has been demonstrated in a large variety of applications and parameters. Examples are the amplification of ultra-low bandwidth emission of non-planar ring oscillators [20], the amplification of nanosecond and picosecond pulses to the multi 100 mJ level [47] and the amplification of femtosecond pulses to more than 1 kW average output power [54].

II. Fundamental Design and Function

The Innoslab amplifier consists of two key components. Firstly, a partially end-pumped slab crystal and secondly an amplifier resonator, which folds the laser beam several times through the pumped volume (Fig. 2). The slab crystal has two optical surfaces (z-direction), two large cooled mounting surfaces (y-direction), and two free surfaces (x-direction). It is end-pumped on a rectangular cross section of a high aspect ratio, which only fills a fraction of the crystal in the y-direction and the full width in the x-direction. This geometry matches the characteristics of laser diode bars with the fast-axis in the y-direction and the slow-axis in the x-direction. The terms slow- and fast-axis are used synonymously with x- and y-direction. The short distance between the pumped gain volume and the large cooled mounting surfaces allows for efficient heat removal. The one-dimensional heat flow in the y-direction establishes a homogeneous cylindrical thermal lens and avoids depolarization by birefringence. Parasitic lasing is suppressed by the grinding of the mounting and free surfaces.

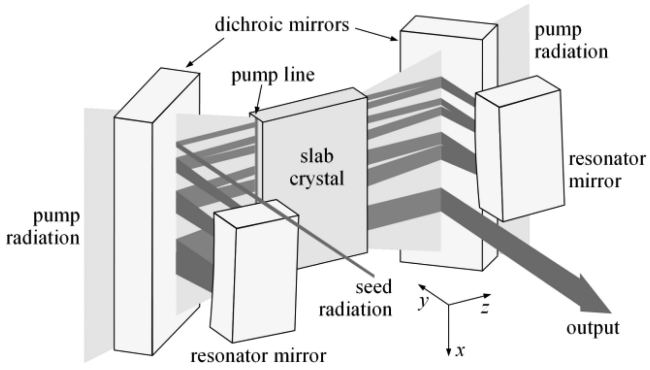

Fig. 3. Depiction of an Innoslab amplifier resonator with two dichroic folding mirrors for the collinear superposition of the pump radiation [52].

The hybrid amplifier resonator is a stable one in the small dimension of the gain volume, which is sustained by the thermal lens and the amplification profile. In the large dimension no thermal lens or gain profile shape the amplified beam, but the amplifier resonator does. Here, a confocal arrangement is normally used, which yields a beam expansion by a constant factor or magnification *M* at each round trip through the resonator (Fig. 2). Additionally, the beam diameter grows due to the beam's divergence. Consequently, plane mirrors in unstable as in stable direction can also be used if the divergence is properly controlled.

The increase in beam cross section by the beam expansion in the unstable direction balances the power increase at amplification and keeps the intensity roughly constant. Besides the thermal management, this beam expansion is a key feature of the concept, because it yields a constant saturation and therefore efficient operation while simultaneously keeping the intensity evenly away from damage thresholds and allowing for small nonlinearity. Although multiple passes through the crystal are accomplished, it is still a single-pass amplifier, because a new section of the pumped volume is saturated at each pass, thereby collecting the smallest possible aberration per overall gain.

For high overlap efficiency the beam matches the pumped volume in the stable direction. In the unstable direction the profiles for the subsequent passes partially overlap in the crystal for efficient operation and to avoid beam deformation due to inhomogeneous gain. The distance between subsequent passes on the resonator mirrors is twice as large as in the slab crystal, if it is located in the center. This permits reasonably separated beams for input and output coupling to the resonator.

The slab crystal is end-pumped and therefore the pump radiation has to be superimposed on the laser radiation with one dichroic mirror, or two in case of pumping from both end faces. This can be a resonator mirror or an additional dichroic folding mirror (Fig. 3). The seed beam is geometrically coupled into the resonator. It can be coupled in and out next to the (sharp) edge of a resonator mirror, exploiting the best beam separation, or with one or two additional scraper mirrors. These are necessary if a resonator mirror is used as dichroic mirror for pumping. In this case the beam has to be coupled in and out at the opposing resonator mirror.

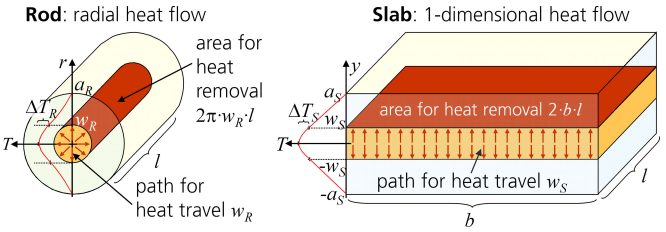

Fig. 4. Heat conduction in rod and slab geometry.

III. Distinctive Properties

A. Thermal Management

The geometry of the slab crystal allows for a reduction of thermally induced aberration compared to other geometries of laser media. For an elementary comparison, the established end-pumped rod geometry is selected, and the following simplifying assumptions are made. The temperature on the cooling surface is constant, the radius of the pumped volume equals the laser beam radius, the thermal load is evenly distributed over the pumped volume, and the heat conductivity is constant and isotropic. Then the heat flow will be strictly radial in the case of rod geometry and one-dimensional in the case of slab geometry (Fig. 4).

The thermal lens induced by the temperature profile and the thermo-optic coefficient χ has the focal length f_R for the rod and f_S for the slab respectively:

$$f_R = \frac{K}{P_h \chi} \cdot 2 \cdot \pi w_R^2, \quad f_S = \frac{K}{P_h \chi} \cdot 2 b w_S. \tag{1}$$

Here, P_h is the thermal load, *K* is the heat conductivity and the meaning of the geometrical parameters is depicted in Fig. 4. The thermo-optic coefficient χ summarizes the change of the index of refraction by temperature *dn/dT* and thermally induced surface deformations and stress [14]. The focal length scales with the pumped area in both geometries. Due to the 2-D heat conduction, the curvature of the temperature profile and focusing power is half as large for the rod as long as the heat density is the same.

The maximum temperature shift in respect to the cooling surface with the crystal length *l* is

$$\begin{aligned} T_R &= \frac{P_h}{4Kl} \cdot \left(1 + 2\ln\left(a_R/w_R\right)\right)/\pi, \quad \text{for rod} \\ T_S &= \frac{P_h}{4Kl} \cdot \left(2a_S - w_S\right)/b, \quad \text{for slab.} \end{aligned} \tag{2}$$

This temperature shift must be below a critical value for efficient laser operation, but it does not determine the thermal aberrations.

To quantify and compare the thermally induced aberrations we make the reasonable assumption, that phase deformations are proportional to the thermally induced phase difference $\Delta\phi$ between the center and the edge of the laser beam acquired at one pass through the crystal. In this context the total phase difference $\Delta\phi$ is typically in the order of π. Beam quality degradations can be characterized by the phase aberrations, which are much smaller than π. The phase difference $\Delta\phi = kl\chi \cdot \Delta T$ is

proportional to the temperature difference ΔT between the center and the edge of the pumped volume for rod and slab:

$$\Delta T_R = \frac{P_h}{8Kl} \cdot 2/\pi, \quad \Delta T_S = \frac{P_h}{8Kl} \cdot 2w_S/b$$
$$\Delta \phi_R = P_h \frac{k\chi}{8K} \cdot 2/\pi, \quad \Delta \phi_S = P_h \frac{k\chi}{8K} \cdot 2w_S/b. \tag{3}$$

The temperature and phase difference is independent of the pumped area for the rod and it scales with the aspect ratio $b/(2w_S)$ of the pumped area for the slab. The phase differences are related by $\Delta\phi_S/\Delta\phi_R = 1.6 \cdot 2w_S/b$. They are determined by the distance for the heat to travel and the area for heat removal. In a rod these terms scale equally with the pump radius, while in a slab the area for heat removal is increased and the distance for the heat to travel is simultaneously decreased by increasing the aspect ratio of the pump area (Fig. 4). As a consequence, a high aspect ratio $b/(2w_S)$ of the gain volume reduces the thermally induced phase difference $\Delta\phi$ and thereby the thermally induced aberrations in the slab geometry. For the scaling of Innoslab amplifiers the results can be easily conceived. An increase of the slab width *b* does not somehow affect the thermal conditions.

B. Beam Expansion

The optical path inside an Innoslab amplifier undergoes a beam expansion during amplification. This expansion is favorable for all kinds of amplifiers as it balances the opposing requirements for efficiency, optical load and beam quality. An efficient power or energy extraction requires an intensity or fluence throughout the laser crystal, which is several times the saturation intensity or saturation fluence. On the other hand, the optical load of the surfaces of the laser crystal limits the intensity and fluence to a fraction of the damage threshold. To balance both, the cross section inside the laser crystal has to be adapted according to the increasing average power.

To improve the beam quality of the amplified beam, wavefront distortions have to be minimized, in particular if there is no spatial filtering. Wavefront distortions are induced by the thermal load of the laser crystal. As described in Section III-A phase aberrations scale with pump power at a given amplifier geometry. The smallest wavefront distortions are gathered up in the gain volume if it is saturated by a single pass. This favors a single-pass amplifier firstly and also implies beam expansion for the reasons discussed before. Innoslab amplifiers inherently fulfill both requirements.

C. Beam Shaping

The beam profile of an Innoslab amplifier is fundamentally different in the slow-axis and fast-axis (*x*- and *y*-direction in Fig. 2). In the fast-axis a Gaussian beam profile can be achieved as in a rod-based laser by proper mode matching. In the slow-axis, geometrical access to the unstable resonator formed by the two mirrors in Fig. 5 always implies truncation and spatial filtering of the in- and out-coupled beam. This results in a *sinc*-like beam pattern in the far-field, shaped by the obstructing edges of the right mirror in Fig. 5 and the laser crystal [52]. At the input, diffraction at the edges can be minimized by increasing the distance $\delta_{\mathrm{in}} w_{\mathrm{in}}$ of the in-coupled beam of radius w_{in} to the diffracting edge. But the situation is much more complex for the out-coupled beam. During amplification the beam profile is influenced by the distance $\delta_n(w_n + w_{n+1})$ of adjacent beams *n* and *n*+1 in the laser crystal. Because the gain is strongly saturated at the beam center, the gain at this position is lower compared to the edges of the amplified beam. This effect is mitigated, however, by the overlap of adjacent beams. Large distances of adjacent beams $\delta_n(w_n + w_{n+1})$ result in a widening and deformation of the beam profile and only a marginal reduction of diffraction at out-coupling and vice versa [52].

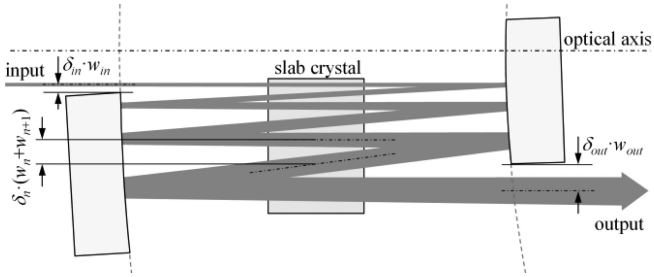

Fig. 5. Geometric beam path of an Innoslab amplifier in the slow-axis.

The consequence is a complex interplay of several factors: the number of passes, magnification, input beam parameters and beam profile, distance to the edges at incoupling and overall gain. Properly balanced, beam deformation by gain saturation is negligible. However, a prominent *sinc*-like diffraction pattern at out-coupling cannot be completely avoided, but can be minimized. When an additional spatial filter is used, the beam profile and beam quality can be easily improved (Fig. 20) with only a small loss of power.

D. Amplifier Properties

Based on the design considerations discussed before, the following characteristics have to be emphasized:

- — Simple single-pass amplification (Fig. 2).
- — High intrinsic efficiency due to a good overlap of amplified mode and pumped volume.
- — Uniform margin of intensity and fluence inside the amplifier to damage thresholds due to mode expansion during amplification.
- — Good beam quality on account of good thermal management.
- — Diffraction pattern in far field can be removed by spatial filtering with small power loss (Section VII-D-3).
- — Scalability in the slow-axis direction without deteriorated thermal management, efficiency and beam quality.
- — Restricted scalability in fast-axis due to deterioration of thermal management.
- — High overall gain due to the folded beam path.
- — High excitation level of the gain medium.
- — Short beam path inside the gain medium.
- — Small B-integral.
- — Very compact setup.

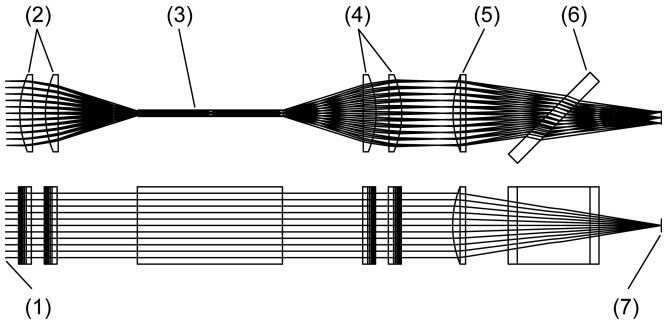

Fig. 6. Principle layout of the Innoslab pump optics in slow- (top) and fast-axis (bottom) direction, with the optics consisting of diode laser stack (1), slow-axis focusing cylindrical group (2), light mixing duct (3), slow-axis collimating cylindrical group (4), fast- and slow-axis focusing group (5), dichroic mirror (6) and focal plane (7).

IV. Optics for Pump Radiation Delivery

The beam quality of high power diode laser stacks is significantly lower in the slow-axis direction compared to the fast-axis direction. Therefore, the fast-axis is commonly focused onto a plane located close to the entrance surface of the slab crystal to be pumped (focal plane), while the slow-axis is homogenized to achieve a top-hat intensity distribution which is typically 10 to 100 times wider than the Gaussian fast-axis intensity distribution. Thanks to the top-hat distribution in the slow-axis direction a temperature gradient inside the crystal in this direction can be avoided. In addition, the homogenization reduces the effect of degradation of single emitters or bars and thereby increases the reliability of the overall system.

To homogenize the slow-axis, the far-field intensity distribution is segmented by a light mixing duct, and the segments are overlaid in the exit plane of the duct [15], [16]. The divergence of the slow-axis is increased by focusing it onto the entrance surface of the light mixing duct. Thereby, a sufficient number of reflections for homogenization of the slow-axis intensity distribution can be achieved with a short light mixing duct. The exit surface of the light mixing duct is imaged in the slow-axis direction on the fast-axis' focal plane. The pump optics consists of five groups as shown in Fig. 6, namely, the cylindrical focusing group (2), the light mixing duct (3), the cylindrical slow-axis collimation (4) and the spherical fast-axis and slow-axis focusing group (5). The dichroic mirror (6) is used for separation of the laser beam.

The magnification of the slow-axis imaging optics is determined by the ratio of the slab's and light mixing duct's widths. The effective focal length of the focusing group is given by the desired pump height as well as the fast-axis divergence and size of the diode laser stack. Depending on the effective focal length of the focusing group and the back focal length, which is defined by the size of the dichroic mirror, a retrofocus configuration can be chosen for the focusing group.

V. Numerical Simulation of Innoslab Amplifiers

Theory and simulation of physical processes is crucial for guiding and interpreting experiments. Beam profile development and amplification in Innoslab amplifiers are complex and intrinsically spatially inhomogeneous processes which makes an analytical treatment virtually impossible, so only numerical methods are likely to yield valuable results.

The first numerical simulations of laser oscillators were published by Fox and Li [17]. The basic procedure of numerically propagating the light beams through the optical system and treating amplification by sheets of amplifying media is still being employed in laser simulations. Besides the seminal work of Fox and Li other methods such as the beam propagation method and finite element method have been developed.

The main prerequisite of the Fox and Li scheme is the assumption of full coherence, which is violated in general in high Fresnel number oscillators. With the input beam being fully coherent, however, the coherence of the beam passing the amplifier is preserved except for noise introduced by spontaneous emission and ASE (amplified spontaneous emission). The main challenge in simulating the propagation of light fields in Innoslab amplifiers is the large effective Fresnel number. The geometric Fresnel number is given by $F_{\mathrm{geom}} = b^2 / (\lambda L)$, with b the larger transverse dimension, L the propagation length and λ the wavelength. For the effective Fresnel number, significant for numerical propagation, the effective dimension $a_{\mathrm{eff}} = \alpha L$ has to be employed, with α the angle between the mirror surface normal and the propagation direction. With $\alpha = 5^\circ$, $L = 100\ \mathrm{mm}$ and $\lambda = 1\ \mu\mathrm{m}$ $F_{\mathrm{eff}} = 760$. The phase on the mirrors changes by $F_{\mathrm{eff}} \cdot 2\pi$ across a_{eff}. As a rule of thumb, at least 10 grid points per 2π phase change have to be taken for the simulation grid in order to get sufficient resolution to describe the light field. Even in a 2D-simulation up to several 10 000 grid points have to be used and with 3D-simulations this number has to be multiplied by a factor of 50 to 100.

The propagation through the amplifying crystal is subject to aberrations caused by temperature- and stress-induced index variations. The absorbed pump power is only partly transferred to the amplified light field, the rest is dissipated to heat. The conversion efficiency is not a constant but, in addition to other factors, depends on the local light intensity, which implies spatial variations of the dissipated heat and temperature. This leads to temperature-induced mechanical stress, with the largest stress values at the edges of the crystal. The index of refraction is a function of both temperature and stress. Although the index variations are dominant perpendicular to the beam propagation direction, the numerical step size within the crystal has to be sufficiently small in order to account for the index-induced phase aberrations during propagation.

In the simulation of cw amplifiers the light field, temperature and stress can be computed iteratively until a steady state has been established. Some numerical results for Innoslab amplifiers can be found in [52]. In pulsed systems this no longer works. In this case light field, temperature and stress have to be computed time-dependently. Together with the required high spatial resolution this results in high computation times. If all the effects discussed here are to be taken into account, efficiently implementing all the computing modules is crucial to make the numerical simulations relevant for developing and improving Innoslab amplifiers.

VI. Design Layouts

The basic layout described in Sections II and III can be further differentiated into amplifiers optimized for cw or high repetition rate, quasi continuous wave (QCW) or burst mode amplifiers, amplifiers with a high energy extraction per pulse and amplifier chains:

A. Continuous Wave and High Repetition Rate

Amplifiers for cw operation or those for pulse trains with repetition rates much higher than $1/\tau_u$ with τ_u as the upper state lifetime are primarily optimized for a high efficiency at high overall gain. This translates into high pump intensities, so that a high gain can be achieved, and into laser intensities during amplification well above the saturation intensity $I_{\mathrm{sat}}(\lambda_l)$ at the lasing wavelength λ_l, so that a high efficiency can be achieved. In the case of 3-level and quasi-3-level laser systems such as Yb:YAG pump intensities have to be well above the saturation intensity $I_{\mathrm{sat}}(\lambda_p)$ at the pump wavelength λ_p. Pump intensity and laser intensity are limited by the brightness or radiance of the pump source and the damage threshold of the laser crystal and coatings involved. Heat removal is not an issue in most cases, but the short focal length of the cylindrical thermal lens is.

The balance between efficiency and damage threshold results in a target pump intensity. At a given pump intensity, the thermal lens in fast-axis results in a favorable (maximal) pumped line height $2w_s$ (Fig. 4). The scaling of the average power is achieved by the slab width *b* only. The gain is adjusted by the number of passes throughout the laser crystal. The overall gain is generally limited to a factor of approx. 10^3 by the onset of parasitic oscillations inside the unstable resonator of the amplifier.

B. Quasi Continuous Wave and Burst Mode

QCW or burst mode involves a pulsed pump source in this context. This gives additional design freedom of the amplifier geometry. At a given intensity of the pulsed pump source, the thermal load, aberration and lens can be reduced by the duty cycle. This can be used to scale the pumped area in fast-axis and by that the average power during the amplification period without compromising efficiency and beam quality.

C. High Pulse Energy

High pulse energies (mJ and higher) imply a significant temporal variation of inversion and gain inside the laser crystal. Energy is stored inside the laser crystal during a pump period in the order of the upper state lifetime and is released by the amplification of a single laser pulse. To store as much energy as possible, the pulse interval of these laser systems lasts longer than the upper state lifetime τ_u, which is typically in the range of 100 μs to 10 ms. For this kind of operation, two additional constraints arise by increased requirements to prevent optical damage and parasitic oscillations.

For high energy extraction and efficiency, a fluence of the amplified pulse is necessary inside the laser crystal in the order of the saturation fluence $F_{\mathrm{sat}}(\lambda_l)$. This is opposed to the damage threshold of the laser crystal and the optical coatings, which therefore limits the extraction efficiency and storable energy.

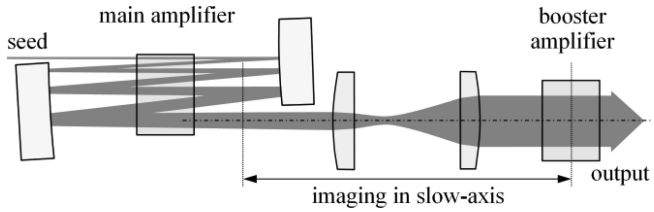

Fig. 7. Conceptual design of adding a booster stage to an amplifier chain.

Because the pump period occurs before the pulse amplification, parasitic oscillations start without competition from the pulse amplification. The stored energy for the pulse amplification and the extraction efficiency are reduced. This gives a limit for the storage-gain along the amplification path of about 1000 and a compromise between extraction efficiency and overall gain.

D. Amplifier Chain

Innoslab amplifiers can be supplemented by further amplifier stages to increase power, pulse energy and gain. This can also be achieved by increasing the crystal width *b* together with a higher number of passes in a single stage. But from a certain power, amplifier chains composed of standardized building blocks are simpler. Innoslab amplifiers with the same folded beam path can be cascaded. The more convenient way is to truncate the incoming beam by the geometric in- and out-coupling of the first stage once and to develop the additional stages into booster stages without additional geometrical truncation (Fig. 7). These booster stages can be viewed as an addition to the last pass of the first amplifier by imaging the truncated output beam of the first stage in the slow-axis to the laser crystal of the booster stage(s). In the fast-axis the same propagation as between successive passes inside the first stage can be achieved by similar imaging optics.

The difference to an Innoslab amplifier with folded beam path is that a spatial filtering or feed-back by edges or overlapping of adjacent beams in the slow-axis is absent. Hence gain saturation tends to shape the beam into a top-hat profile inside the booster amplifier, increasing side lobes in the far-field. All other properties of the initial setup are preserved.

VII. Achievements

A. Single-Frequency Amplifier

Nonplanar ring oscillators (NPRO) based on monolithic laser crystals are state-of-the-art sources for the generation of single-frequency emission at comparably high output power. About 1 kHz/100 ms bandwidth at relative intensity noise level (RIN) below $1 \cdot 10^{-5}$ $\mathrm{Hz}^{-1/2}$ without and $1 \cdot 10^{-7}$ $\mathrm{Hz}^{-1/2}$ with active noise suppression are available at up to 2 W cw output power. The center wavelength of the NPRO can be tuned over a range of 30 GHz. The beam quality factor is $M^2 = 1.1$. Higher output power of the NPRO oscillator results in thermo-optical effects

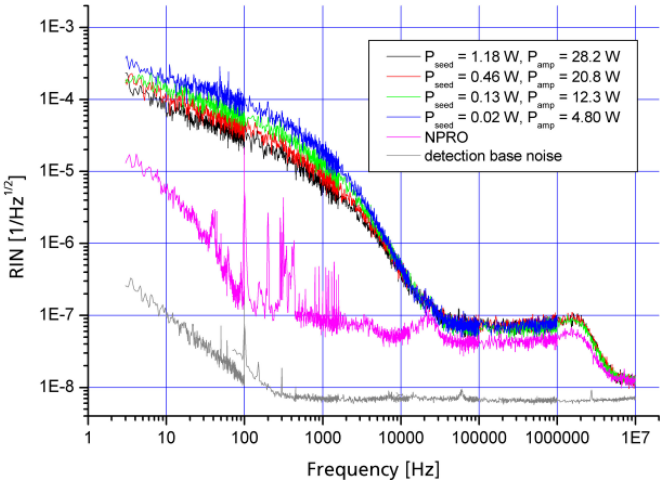

Fig. 8. RIN measurement of NPRO and Innoslab amplifier [20].

[18], [19]. However, extremely sensitive interferometers and other fundamental research experiments as well as efficient cw frequency conversion for commercial applications require much higher output power. To achieve an output power of 40 W an Innoslab amplifier was adapted to the 1.2 W output power of an available NPRO [20]. A configuration with 4 beam passes was selected in combination with a 10 mm $\times$ 10 mm $\times$ 1 mm Nd:YVO_4 crystal as gain medium.

The large surfaces of the slab laser crystal are soldered to a water cooled heat sink. There is no contact of the cooling water to the crystal. This configuration reduces the introduction of acoustic noise by the water flow to the amplified signal. We demonstrated that the Innoslab amplifier adds almost no noise to the NPRO signal above a frequency of 10 kHz and less than 10 dB at lower frequencies (Fig. 8). Frequency tuning over the full NPRO range of 30 GHz results in an output power variation below 7%.

B. ns-Amplifier

The Innoslab architecture has successfully been applied to amplifier stages in the nanosecond pulse duration regime. The development started about ten years ago mainly for applications in the field of materials processing. Here, high average power, high repetition rate up to the 100 kHz range and high beam quality are important design drivers.

The development of laser sources for airborne and spaceborne LIDAR applications in the field of atmospheric research started a few years later. Here, lower repetition rates below 1 kHz but higher pulse energies of several 10 mJ at high beam quality, very high efficiency and robustness are crucial design drivers. Usually, single- or double-pass amplifiers are used in this parameter regime where the architecture is based on side-pumped rods [21] or zigzag slabs. Side-pumping usually leads to compact pump setups but to low overlap efficiencies. The Innoslab architecture offers a very good combination of high efficiency at moderate and constant fluences, high beam quality and compactness to meet these stringent requirements.

If the exact emission wavelength is not an important requirement as in optical parametric oscillator (OPO) pumping, Nd:YAG is typically chosen as the active medium for LIDAR systems. For direct wavelength generation, the Innoslab architecture can be adapted to the needs of more unfamiliar laser crystals, which are compositionally tuned to the application wavelength. This was successfully done for the development of laser sources at 935 nm wavelength for water vapor DIAL (Differential Absorption LIDAR) instruments.

All these kinds of systems will be described further. An overview of the main optical properties of different amplifier stages is given in Table I.

1) Nd:YAG Laser at 1064 nm for LIDAR Applications: Development started with a pre-development laboratory model of the ATLID laser source for the spaceborne atmospheric backscatter LIDAR instrument named ATLAS [4] developed for the ESA (European Space Agency). Based on this setup, three tailored pump-laser sources were developed for the airborne LIDAR systems A2D2G and CHARM-F [22]. A2D2G is designed to measure wind profiles based on the Doppler shift of the backscattered photons at 355 nm of the frequency tripled pump source at 1064 nm. CHARM-F will be used to measure column-averaged volume mixing ratios of CH_4 and CO_2 measured by integrated path differential absorption (IPDA). The light pulses at the measurement wavelengths of 1645 nm and 1572 nm, respectively, are generated in OPOs or optical parametric amplifiers (OPA).

All three airborne laser sources (A2D2G, CHARM-F-CH_4, CHARM-F-CO_2) have an identical optical architecture up to the first Innoslab amplifier stage, which is very similar to the ATLAS setup. A Q-switched stable oscillator that is injection seeded and cavity controlled generates laser pulses of 30–40 ns pulse duration at about 8 mJ of pulse energy and nearly diffraction limited beam quality [4], [22]. In both CHARM-F-lasers pulse pairs with 500 μs temporal separation between both pulses are emitted at 50 Hz repetition rate. This is required for low error IPDA measurements of fast varying measurement volumes. In case of A2D2G and ATLAS single pulses with 100 Hz repetition rate are emitted. The pulses are amplified in a seven-pass Innoslab amplifier stage to about 85 mJ of pulse energy. In the A2D2G and CHARM-F-CO_2 system these pulses are amplified to about 150 mJ pulse energy in a second two-pass Innoslab stage. The principle optical setup is depicted in Fig. 9. Typically, the amplifier stages have an optical to optical efficiency of 20 to 25% when the pump light after all pump optics as input energy and the extracted pulse energy as the output are taken into consideration. The transfer efficiency of the pump optics has to be considered separately.

For all amplifier stages Nd:YAG slab crystals with an optical aperture of 18 mm $\times$ 4 mm, a length of 20 mm and a Nd-doping level of 0.7 at% are used. The slabs are pumped at a height of about 1.8 mm by beam-shaped commercially available passively cooled fast-axis collimated diode stacks. The thermal lens in the fast-axis direction has a focal length of about 3 m at the working point according to calculations at 100 Hz repetition rate and 50 Hz dual pulse operation. The geometrical length of one amplifier pass for all systems is 100 mm. A geometrical magnification $M = 1.4$ is applied to the beam in the seven-pass

TABLE I
INNOSLAB AMPLIFIERS WITH <100 ns PULSE DURATION

Laser system		Host of Nd	Pulse energy	Pulse duration (FWHM) repetitionrate	Beam quality M^2	o-o efficiency[a]
Seven-pass *ATLAS*[d]	[4]	YAG	85 mJ	30 ns 100 Hz	1.55 × 1.35	0.247
Seven-pass[c] *CHARM-F* CH_4 [e]	[22]	YAG	85 mJ	30 ns 2x 50 Hz	1.6 × 1.4	0.237
Seven-pass[c] First stage *CHARM-F* CO_2 [e]	[22]	YAG	85 mJ	30 ns 2x 50 Hz	no data	0.144[b]
Two-pass[c], second stage *CHARM-F* CO_2 [e]	[22]	YAG	150 mJ	30 ns 2x 50 Hz	1.6 × 2.0	0.123[b]
Seven-pass, first stage *A2D2G*[e]		YAG	89 mJ	30 ns 100 Hz	no data	0.2
Two-pass, second stage *A2D2G*[e]		YAG	160 mJ	28 ns 100 Hz	1.7 × 1.7	0.196
13-pass *EMMA*[d]	[27]	YGG	31 mJ	53 ns 100 Hz	1.18 × 1.36	0.032
Six-pass	[30]	YVO_4	3.8 mJ	5 ns 1 kHz	1.3 × 1.3	0.03
Six-pass	[30]	YVO_4	0.7 mJ	14 ns 50 kHz	1.3 × 1.3	0.25
Six-pass single crystal MOPA	[29]	YVO_4	0.29 mJ	15 ns 100 kHz	1.3 × 1.3	0.225
Four-pass[d]	[31]	YAG	12 mJ	28 ns 10 kHz	3.0 × 1.4	no data

[a]pump energy behind all pump optics to extracted energy; [b]nonrepresentative low efficiencies due to low spectral overlap of pump radiation and absorption; [c]double pulse operation at 50 Hz repetition rate, time between double pulses: 500 μs; [d] laboratory model; [e] designed for airborne application.

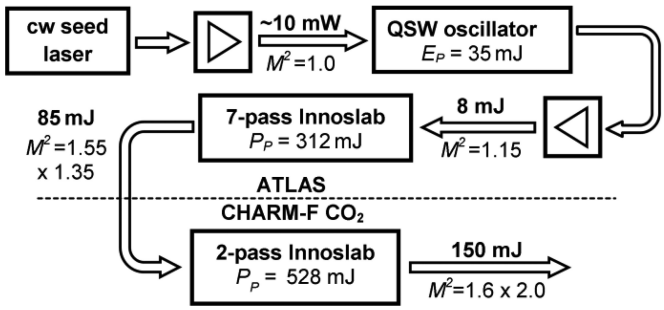

Fig. 9. Schematic setup of Nd:YAG-based single-frequency Innoslab MOPA at 100 Hz repetition rate. Up to the end of the first amplifier stage all setups (ATLAS, CHARM-F-CH_4, CHARM-F-CO_2, A2D2G) have very similar properties [4], [22]. The representative values of the ATLAS system are presented here for the oscillator and first amplifier stage. For the second amplifier stage the values of the CHARM-F-CO_2-system are considered [22].

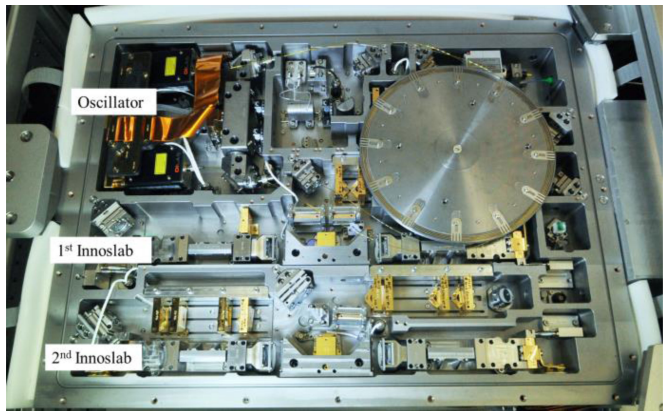

Fig. 10. Pump-laser section of the CHARM-F-CO_2-system including the Q-switched single-frequency oscillator and two Innoslab amplifier stages. The setup has a footprint of 500 mm x 834 mm, including the harness connector box not shown here. (The disc that covers oscillator section on right-hand side is a fiber spool for the safe storage of the passive transport fibers for the oscillator pump radiation.).

case. Due to the low amplification factor of about 2 no beam expansion is applied between both passes of the two-pass booster stage. The peak fluences are in the range of 4–6 J · cm^{-2} for all passes, which is well below typical damage threshold values. This is crucial for long lifetimes.

Beside efficiency and beam quality the spectral beam properties are essential for many LIDAR applications. For the ATLAS amplifier stage the spectral width before and after the amplifier was measured with the heterodyne technique [4]. The pulse duration of the oscillator is 36 ns (FWHM), the spectral line width 15 MHz (FWHM) and the TBP (time-bandwidth-product) 0.49. For the 7-pass amplifier stage the pulses are shortened to 30 ns at a spectral line width of 17 MHz, but the TBP of 0.51 is virtually conserved by the Innoslab amplifier stage.

The pump-laser section of the CHARM-F-CO_2 system including the oscillator and both amplifiers is depicted in Fig. 10. The frequency converter stages will be mounted on the opposite side of the laser plate.

2) Nd:YGG-LIDAR at 935 nm: In a feasibility study for spaceborne water vapor DIAL systems the adaption of Innoslab amplifiers to different crystal material is currently being investigated. The relevant absorption lines around 935 nm can be addressed by Nd:YLuGG $((Y_x Lu_{1-x})_3 Ga_5 O_{12})$ mixed garnet crystals with the composition x $\sim$ 0.58 [23], [24]. The properties of such a laser source have been theoretically and experimentally analyzed in a laser based on Nd:YGG, which is a Nd:YLuGG-crystal with the special composition $x = 1.0$ [24]–[27] and having similar properties to the fine-tuned composition. The main drawback of these materials is the emission cross section of about 1.5×10^{-20} cm^2 at 935 nm which is about a factor of 17 smaller than in Nd:YAG at 1064 nm. Some further disadvantages are strong thermal lensing and the risk of parasitic lasing at 1062 nm, with a ten times larger emission cross section than at 935 nm and reabsorption due to the quasi-3-level characteristics. The design of the Innoslab amplifier has to be adapted to these crystal properties to perform properly. Due to the small emission cross section, the efficient energy extraction needs higher fluences and, therefore, smaller spot sizes and more passes through the gain medium.

The schematic setup is depicted in Fig. 11. Nearly diffraction limited pulses of 4.3 mJ pulse energy at 50 ns pulse duration are generated in a rod-based, stable, Q-switched, injection seeded oscillator at a repetition rate of 100 Hz. The pulses are amplified in a 13-pass Innoslab amplifier to about 30.5 mJ. For this amplifier stage a slab crystal is used with an optical aperture

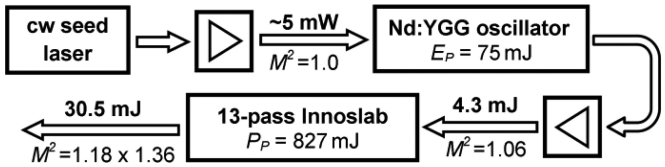

Fig. 11. Nd:YGG-based MOPA system at 935 nm designed for water vapor DIAL systems [27].

of 14.8 mm × 2 mm, a length of 15 mm and a Nd-doping concentration of about 0.8 at%. It is partially pumped at a height of 0.9 mm. The geometrical length of one amplifier pass is 70 mm. The thermal lens in the fast-axis direction has a focal length of 225 mm at the operating point. Due to the low amplification factor, both resonator mirrors of the amplifier are plane in the slow-axis and the beam is only expanded by divergence in the slow-axis. In order to match the laser mode to the pump height, the mirrors are convex in fast-axis. In comparison to the saturation fluence of 14 J · cm^{-2}, the peak fluence of 2–5 J · cm^{-2} for all crystal passes is low, increasing with the pass number. Due to the low fluences the optical-optical efficiency is about 3.2% and much smaller than for Nd:YAG Innoslab amplifiers at 1064 nm, but is comparable to laser systems based on efficiently pumped OPOs or Ti:Sapphire lasers at 935 nm of about 3–4% [24].

The Nd:YGG setup was successfully used in ground-based water vapor DIAL measurements, where excellent spectral purities of better than 99.996% could be demonstrated [28]. The spectral bandwidth is <28 MHz (peak value) and <14 MHz (mean value) [27], and the TBP 0.73.

While it was shown that this kind of laser concept can meet the stringent requirements for water vapor DIAL measurements two main issues have to be clarified and experimentally proven for a spaceborne water vapor DIAL system. Firstly, the Nd:YGG-crystals have to be replaced by spectrally tuned Nd:YLuGG crystals with the composition $x \sim 0.58$ in order to address spectrally all relevant absorption lines. Secondly, the pulse energy has to be doubled for example in a subsequent amplifier stage. Currently, both issues are being investigated.

3) Outlook: Presently, the Nd:YAG-based systems are being further developed for spaceborne systems consisting of an oscillator and one Innoslab amplifier stage. While the optical architecture can be transferred from the airborne systems, the mounting technology has been improved in order to fulfill the strong requirements for robustness and lifetime.

As the quality of most of the LIDAR measurements depends more on the pulse energy than on the repetition rate, the scalability of individual Innoslab amplifier stages to higher pulse energy up to the Joule level is being investigated.

The direct generation in tailored crystal materials such as Nd:YGG is a promising technology for further applications. For example, the methane absorption lines at 1645 nm have been successfully addressed in Er:YLuAG crystals [32], [33] and Ho:YLF is a promising candidate for CO_2 IPDA measurements at 2051 nm [34]. This requires a detailed design of all relevant Innoslab amplifier properties matched to the particular crystal material.

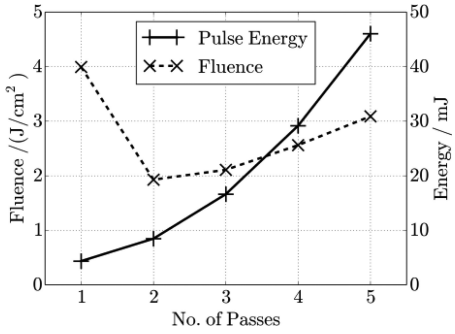

Fig. 12. Calculated pulse energy and fluence for each of the five passes in the Ho:YLF Innoslab amplifier.

4) Er/Tm/Ho-Innoslab Amplifier: The good matching of Innoslab amplifiers to brilliant high power diode lasers enables high pump intensities throughout the gain volume. Therefore, the Innoslab concept is particularly beneficial for resonantly pumped laser materials with emission in the IR-B spectral band, i.e. Er^{3+}-doped crystals at 1.6 μm and Ho^{3+}-doped crystals at 2 μm emission wavelengths. Because of the thermal population of the lower laser level, high inversion levels are required along the length of the crystal. These dopants exhibit small emission cross sections in this spectral region on the order of 5×10^{-21} cm^2 and suffer from significant upconversion effects which limit the feasible doping level to below 1% [35], [36]. This results in laser crystal lengths of 50 mm and more and in low gain.

The small emission cross section corresponds to a large saturation fluence (about 20 J/cm^2 for Er:YAG at 1.6 μm and 4 J/cm^2 for Ho:YLF at 2.0 μm), which needs to be exceeded in order to extract more than about 50% of the stored pump energy in the laser crystal. The Innoslab's degree of freedom in beam expansion over the amplification process is an important asset here.

Bollig *et al*. used an Innoslab-like architecture to generate single-frequency laser pulses at 2 μm with pulse energies of 200 mJ from Ho:YLF and Ho:LuLF slab crystals [37]. In the absence of pump diodes with high spectral and spatial brightness, a Tm-based Innoslab oscillator generating a line-shaped laser beam at 1.9 μm was used for pumping.

Based on the Innoslab architecture, a Tm/Ho-MOPA-chain has been designed for CO_2-LIDAR measurements at 2051 nm. Trains of at least two consecutive single-frequency laser pulses with 40 mJ and 20 mJ are required as the online and offline pulses for differential absorption LIDAR. Up to now the Tm:YLF Innoslab pump laser has been realized and provides 200 W of optical output power at 1.9 μm in cw operation [38].

The amplifier design for the quasi-2-level electronic system is assisted by the simulation of a spatially and temporally resolved solution of the laser rate-equations of both multiplet and Stark-level populations. In Fig. 12, the predicted pulse energy and the fluence on the laser crystal facets are plotted over the number of amplifier crystal pass. While the pulse energy is amplified by an order of magnitude the variation of the fluences is limited to a factor of two. The planned architecture for the Tm/Ho-MOPA is sketched in Fig. 13.

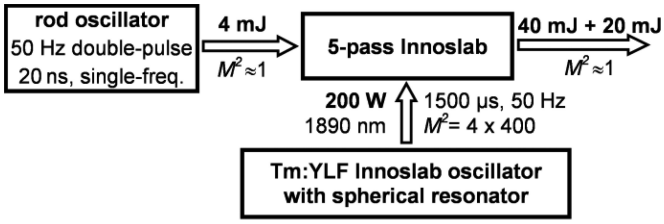

Fig. 13. Schematic setup of the planned Ho:YLF-MOPA at 2 μm for CO_2-LIDAR.

For scaling the pulse energy of single-frequency laser pulses with a wavelength of 1645 nm, a similar Er^{3+}-doped, Lu^{3+}-codoped YAG Innoslab-amplifier is under development. At a repetition rate of 100 Hz pulses of 80 ns duration will be amplified from 3 to 40 mJ.

C. ps-Amplifier

1) High Repetition Rate: For the high speed precision structuring of large surfaces, those may consist of different materials such as steel and ceramics, an almost diffraction-limited picosecond laser of several 100 W is required. Such laser systems have been realized by Innoslab MOPA systems (Table II). For the system shown in Fig. 14, seeding pulses with 10 ps duration at 1064 nm wavelength and 3 W average power are provided by an industrial laser system in MOPA configuration (Lumera Rapid) [39] or an oscillator with Watt level output power. The first system generates a tailored distribution of energy into groups of pulses (pulse trains) at a repetition rate as high as 1 MHz whereas the 10.7 MHz oscillator runs with a fixed repetition rate.

The Innoslab amplifier consists of a 1 mm thick Nd:YVO_4 crystal, 10 mm long and 24 mm wide, which is end-pumped from both end faces by max. 2 × 345 W. The input beam is shaped to an elliptical profile and folded through the amplifier crystal with seven passes. For the amplifier resonator two plane mirrors are used to efficiently extract the stored power in the slab crystal by expanding the beam by its divergence in slow-axis. The output power at 2.67 W seed power is 200 W at 1 MHz repetition rate, corresponding to a pulse energy of ∼200 μJ. By clocking down the MOPA seed source to a 500 kHz repetition rate at 2.31 W seed power an output power of 160 W is achieved without parasitic lasing. For the 10.7 MHz oscillator an output power of 254 W with 33% o-o efficiency is achieved, which is the highest reported power from a single Nd-based amplifier [44]. With a second Innoslab amplifier stage using a 20 mm × 1 mm × 15 mm Nd:YAG slab crystal pumped from both end faces, an output power of 395 W is achieved. The o-o efficiency of 20.3% of the 1-pass booster amplifier can be further improved by tuning the seed source to the amplification bandwidth of the Nd:YAG slab crystal or by using a Nd:YVO_4 crystal as gain medium.

2) Low Repetition Rates: For laser ablation of human tissue in medical surgery, picosecond pulses at 532 nm are advantageous, especially if the tissue is placed in water with a high ion concentration. The short pulse duration reduces the thermal load

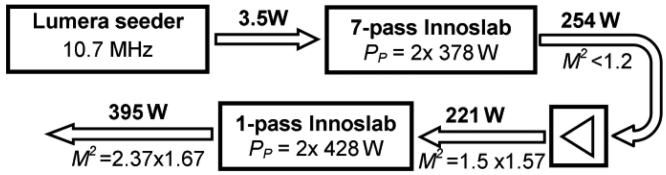

Fig. 14. Two-stage Nd:YVO_4 Innoslab MOPA ps-system.

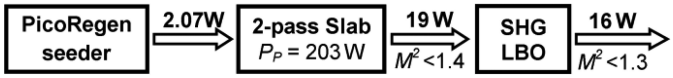

Fig. 15. Nd:YVO_4 Innoslab MOPA ps-system with 25 ps pulse duration and 1.9 mJ pulse energy at 1064 nm and 1.6 mJ at 532 nm.

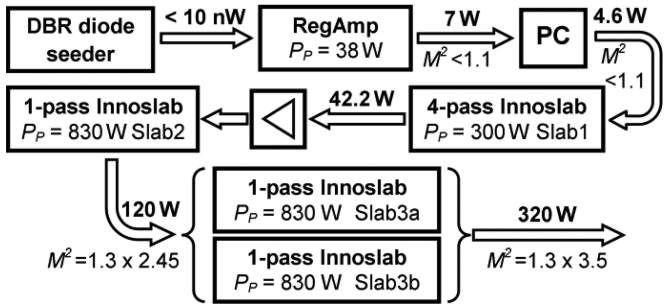

Fig. 16. Four-stage high energy Nd:YAG Innoslab ps-system running at 2 kHz repetition rate. PC Pockels cell; brackets stand for polarization multiplexing.

in the human body, and the absorption of radiation at 532 nm by salt water is smaller compared to radiation at 1064 nm. The objectives for an adequate laser source are energies >1 mJ at 532 nm and pulse durations <50 ps at repetition rates >10 kHz. An appropriate Innoslab-based MOPA has been developed [45].

The seed source consists of an oscillator and regenerative amplifier delivering pulses of 0.17 mJ energy and 10 ps duration (HighQ, PicoRegen). The pulse duration of the oscillator is adjusted to 25 ps using an etalon. The pulses are amplified with a two-pass Innoslab amplifier comprising a 12 mm × 10 mm × 1 mm Nd:YVO_4 crystal pumped from one end face. Nonlinear effects are prevented by the short amplification path. At 203 W pump power a pulse energy of 1.9 mJ at 10 kHz repetition rate is achieved in a very simple and compact setup, at the expense of a reduced o-o efficiency of 9%. Frequency conversion to 532 nm with a 5 mm × 5 mm × 18 mm LBO crystal (Type II at 35 °C) to 1.6 mJ pulse energy was performed (Fig. 15).

For a different application even higher pulse energies with a duration of some 100 ps are needed. Indeed, the biological and medical sectors have a great interest in tabletop XUV or soft-X-ray sources for microscopes in the "water window" (spectral range 2.3–4.4 nm) for organic samples. Laser produced plasma sources for the generation of XUV radiation demand compact laser systems with pulse energies in the order of 100 mJ, pulse durations of 500 ps to 3 ns for high conversion efficiency and repetition rates >1 kHz to achieve short exposure times in the

TABLE II
INNOSLAB AMPLIFIERS WITH ~10-ps PULSE DURATION

Nd:Innoslab amplifier system		Average output power (rep. rate)		Max. pulse energy (rep. rate)		Pulse duration (FWHM)	Beam quality M^2
One-stage	[40]	47 W	(1,5 MHz)			13 ps	1.1×1.4
Five-stage	[41]	422 W	(2 MHz)	0.8 mJ	(0.5 MHz)	11 ps	
One-stage	[42]	46 W	(100 kHz)	0.6 mJ	(30 kHz)	12 ps	
One-stage	[43]	73 W	(80 MHz)			15 ps	1.4×1.6 (60 W)
One-stage	[44]	105 W	(120 MHz)			8.4 ps	1.2×1.09
One-stage	(2011)	254 W	(10.7 MHz)	320 μJ	(0.5 MHz)	11 ps	1.14×1.19
Two-stage	(2011)	390 W	(10.7 MHz)			11 ps	1.67×2.37

range of a few 10 s. A MOPA system consisting of a diode-seeded regenerative amplifier (DSRA) in rod geometry [46] and a chain of four Innoslab power amplifier stages meets this demand (Fig. 16) [47].

The DSRA generates pulses with an energy up to 3.5 mJ and up to 7 W average power at diffraction limited beam quality. The pulse duration can be varied between 250 ps and 1.5 ns. Pre-pulses, which are characteristic for the regenerative amplifier, are amplified disproportionately high in the amplifier chain compared to the saturating main pulse due to the high small signal gain. This significantly worsens the contrast ratio of the entire MOPA. Hence the DSRA's contrast ratio of ~1:1000 is improved by an additional extra-cavity Pockels cell and polarizer. The losses of isolating and pulse picking devices reduce the input seed energy to the Innoslab amplifier chain to about 2.3 mJ.

Slab1 serves as a four-pass pre-amplifier with two plane resonator mirrors. In the fast-axis the beam of the DSRA is transformed by cylindrical lenses to match the gain volume of the 20 mm × 15 mm × 1.6 mm Nd:YAG crystal. To isolate the high gain of Slab1 from the rest of the system, an optical isolator is used. To pass through the Faraday isolator, the elliptical output of Slab1 is transformed by a cylindrical telescope. Behind the isolator the beam is adapted with a second cylindrical telescope to fill the crystal and to extract the stored energy of the booster amplifier Slab2 in one single pass.

Behind Slab2 the polarization is rotated by 45° with a wave plate. A subsequent polarizer splits the beam into two beams, which propagate through Slab3a and Slab3b. Afterwards the two beams are superimposed by noncoherent polarization coupling.

Pulses with a duration between 250 ps and 1.5 ns have been amplified with a single linear chain of three slab amplifiers and with polarization multiplexing on the final stage. With the linear three-stage amplifier chain a total average power of 236 W at 2 kHz and 175 W at 1.3 kHz is achieved, resulting in pulse energies of 118 and 136 mJ respectively. With four amplifiers and polarization multiplexing in the last stage, a total power of 320 W is achieved, resulting in a pulse energy of 160 mJ (2 kHz). The peak power is >500 MW, the beam quality is $M^2 < 1.3 \times 3.5$ and the contrast ratio between amplified pre-pulses of the DSRA and the main pulse exceeds 500:1. All parameters such as power, pulse duration and pulse shape are adjustable via software. Second harmonic generation with one linear amplifier chain has been demonstrated with a conversion efficiency of >50%. At present two lasers are integrated into plasma sources for X-ray microscopy [48]–[50]. One system is the one described above, whereas the second system is a three-stage amplifier chain without polarization multiplexing with a 1.3 kHz repetition rate.

D. fs-Amplifier

1) Design Considerations: To amplify fs-pulses, i.e. pulses with pulse durations <1 ps laser crystals with a sufficient amplification bandwidth are essential. For average powers of more than 100 W, Yb-doped laser materials have become established. The main reasons are the availability of high power and high brightness diode lasers in the wavelength range of $\lambda_p = 940-980$ nm, the high efficiency and the low waste power. Because of the quasi-3-level energy scheme, pump intensities throughout the gain volume in the order of the saturation intensity of the pump radiation $I_{\mathrm{sat}}(\lambda_p)$ are essential.

Since 2007 diode lasers have been developed to such an extent that Innoslab amplifiers based on Yb:YAG can be pumped efficiently. Among ytterbium-doped laser crystals, Yb:YAG provides the highest emission cross section $\sigma_e = 2 \times 10^{-20}$ cm^2, the lowest saturation intensity $I_{\mathrm{sat}}(\lambda_p) = 28$ kW·cm^{-2} at the pump wavelength, the best optical quality and a high heat conductivity $K = 8.6$ W·m^{-1}·K^{-1} (2% doping), but the lowest emission bandwidth $\Delta\lambda \approx 5$ nm as well. Some of the experimental results with Yb:YAG are summarized in Table III.

The basic layout of Yb:YAG Innoslab amplifiers is dominated by its quasi-3-level nature. At room temperature the population of the lower state absorbs laser radiation at the lasing wavelength of $\lambda_l = 1030$ nm. A pump intensity of ~7 kW · cm^{-2} is necessary to attain an amplification of one. The pump intensity has to exceed this threshold intensity by many times in order to take advantage of the otherwise excellent efficiency and gain of Yb:YAG.

Yb:YAG Innoslab amplifiers are pumped at an intensity of $I_p = 30 - 60$ kW · cm^{-2}, which is almost completely absorbed in the gain volume. The pump intensity in combination with a heat fraction $\eta_h = 0.1$, thermo-optic coefficient $\chi = 1 \times 10^{-5}$ K^{-1} [61] and heat conductivity $K = 8.6$ W · m^{-1}·K^{-1} (2% doping) determines the focal length of the cylindrical thermal lens $f_{\mathrm{th}} = 14$–28 mm (1). When gain-guiding is neglected, the focal length limits the length of the hybrid resonator with plane mirrors in fast-axis to $< 4 f_{\mathrm{th}}$. In all the amplifiers realized, an approximate confocal setup in the fast-axis is used for a broad stable operation range and a moderate intensity

TABLE III
INNOSLAB AMPLIFIERS WITH <1 ps PULSE DURATION

Yb:Innoslab amplifier system		Average output power	Pulse energy	Pulse duration (FWHM)	Beam quality[a] M^2
One-stage	[51]	77 W	$1.2\ \mu J$	786 fs	1.27×1.17
One-stage	[52]	400 W	$5.3\ \mu J$	682 fs	1.44×1.28
One-stage with stretcher	[53]	350 W	$3.5\ \mathrm{m}J$	720 fs	1.35×1.25
One-stage	[54]	620 W	$31\ \mu J$	636 fs	1.43×1.35
One-stage	[55]	186 W	$60\ \mu J$	609 fs	1.29×1.13
One-stage	[56]	217 W	$21\ \mu J$	650 fs	1.33×1.30
One-stage with CPA	[57]	160 W	$12.8\ \mathrm{m}J$	830 fs	1.4×1.1
One-stage with CPA	[58]	320 W	$3.2\ \mathrm{m}J$	936 fs	1.2×1.04
Two-stage	[54]	1100 W	$55\ \mu J$	615 fs	2.7×1.5
Two-stage	(2013)	930 W	$46.5\ \mu J$	800 fs	1.42×1.09
Two-stage with spatial filter	(2013)	540 W	$53\ \mu J$	830 fs	1.17×1.06
One-stage with OPCPA	[59]	11.4 W	$3.5\ \mu J$	29.1 fs	?
One-stage with compression	[60]	23 W	$1.2\ \mu J$	35 fs	?
Two-stage with compression	(2013)	375 W	$37.5\ \mu J$	<170 fs	1.38×1.33

Published results until end of 2013 and unpublished results by the authors; [a]Beam quality measured by ISO 11146 and 4σ -method.

on the resonator mirrors. These objectives determine the resonator length of about 35 mm, the height of the pumped volume $2w_s = 200\ \mu$m (Fig. 4) and the pump power per crystal width $P_p/b = 600-1200\ \mathrm{W \cdot cm^{-1}}$. The thermal aberrations are comparable to an end-pumped rod amplifier with pump power $P_p = 20$–40 W (Section III-A). By soldering the slab to the actively cooled heat sink, the surface temperature is kept constant. At a slab length $l = 10$ mm and a slab thickness $2a_s = 1$ mm, a rise in temperature $\Delta T = 16-31$ K (3) occurs. For a pumped area height $2w_s = 200\ \mu$m a pump beam quality in fast-axis of $M^2 = 10$ is required.

It is instructive to compare continuously pumped Innoslab amplifiers based on Yb:YAG to amplifiers of the same average power based on Nd:YAG. The differences mainly arise from the upper-state lifetimes of 950 and 230 μs, saturation intensities of 11 and 1.7 kW $\cdot$ cm^{-2} and saturation fluences of 11 and 0.4 J $\cdot$ cm^{-2} of Yb:YAG and Nd:YAG respectively. For Yb:YAG the following holds:

- — Up to 55% o-o efficiency compared to 40%.
- — An absolute thermal load smaller by a factor of 3.
- — Higher requirements on optical design of pump optics and brightness of diode lasers.
- — Pulses shorter a factor of $\sim$10 by broader bandwidth.
- — Width and height of pumped cross section smaller by a factor of $\sim$3 at the same average power.
- — Intensities on optical surfaces higher by a factor of $\sim$10.
- — Comparable thermal and thermo-optical conditions.
- — Comparable saturated gain.
- — Stored energy higher by factor of 4.
- — Fluence on optical surfaces higher by a factor of $\sim$25 at low repetition rates $\nu_{\mathrm{rep}} < 1/\tau_u$.
- — Repetition rates $\nu_{\mathrm{rep}} < 10$ kHz only partially applicable, in contrast to Nd:YAG.

2) Current State of Technology: Based on the experience with Nd:YAG continuously pumped Yb:YAG Innoslab amplifiers and amplifier chains rapidly evolved to reach an average output power of a kilowatt. Amplification factors of 1000 are routinely achieved in a single Innoslab stage. Saturation of the whole gain medium is ensured by $\sim$5 W seed power. The seed

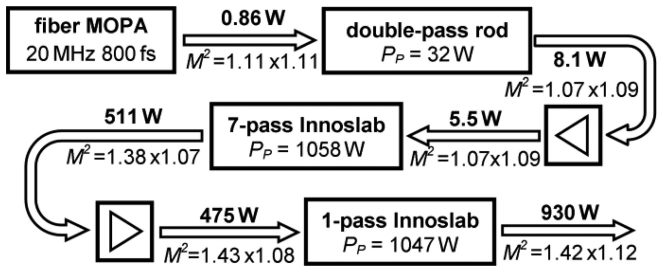

Fig. 17. Two-stage Innoslab MOPA system similar to reference [54].

radiation with a circular beam profile has to be mode matched to the amplifier only in fast-axis. Bandwidth-limited pulses are achieved with an appropriate seed source. When the narrow emission bandwidth of Yb:YAG is taken into account, pulse distortions by dispersion during amplification can be neglected. The B-integral inside the amplifiers limits the repetition rates to $\nu_{\mathrm{rep}} > 10$ MHz or pulse energies of $\sim$50 μJ at pulse-durations <1 ps. At these parameters spectral broadening due to self-phase modulation becomes distinct at B-Integrals of $\sim$3. Higher pulse energies are feasible at the expense of efficiency or pulse duration. Employing chirped pulse amplification enables pulse energies of $\sim$10 mJ or even higher [62]. In Fig. 17 a typical amplifier setup for ultra-short pulses is depicted, which is based on the two-stage Innoslab amplifier described in [54].

The first amplifier stage is completely enclosed (Fig. 18) and can be remotely controlled to protect the highly loaded optical elements (10^{10} W $\cdot$ cm^{-2} peak) from the environment, enabling stable daily operation for months and elimination of beam fluctuations. The total footprint of the complete MOPA system is 1.5 m^2. Compared to reference [54] the beam quality is greatly improved up to $M^2 = 1.42 \times 1.12$ (Fig. 19) due to a good beam quality of the seed source, proper matching of the input beam parameters and a new design of the slab crystal heat sink.

Two amplifier stages with Yb:YAG crystals of dimensions 10 mm $\times$ 10 mm $\times$ 1 mm pumped double-pass from both end faces are used to amplify the seed radiation in seven passes for

Fig. 18. Housed 2-stage Innoslab MOPA of Fig. 17 including spatial filtering, pulse-compression (front) and vacuum-chamber for experiments (right).

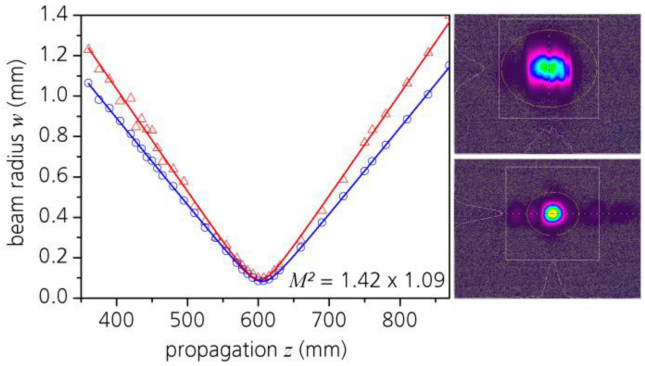

Fig. 19. Beam radius at $P = 930$ W output power of system in Fig. 17 and beam profile at slab crystal (top) and far-field (bottom).

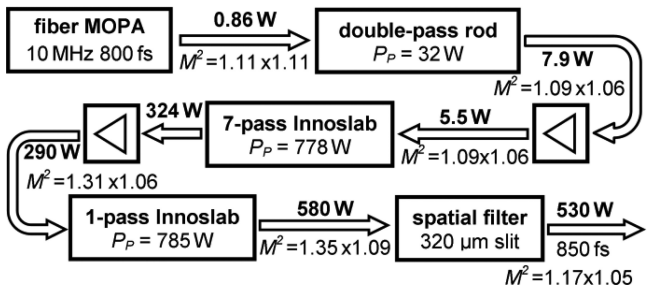

Fig. 20. Spatially filtered Innoslab MOPA system.

the first amplifier stage and one pass for the second. A slab isolator is integrated between the amplifier stages, containing a TGG crystal of dimensions 12 mm $\times$ 14.3 mm $\times$ 1.5 mm. The slab-shaped isolator crystal and one-dimensional heat flow improves the thermal management by a factor of approximately 10 compared to a crystal rod. The reasons are the same as for the gain medium (Section III-A). Thereby, the slab isolator sustains a kilowatt of average power at 35 dB isolation and $>$97% transmission without beam quality deterioration. The output of the first amplifier stage is imaged into the isolator and the isolator into the second amplifier stage, adapting width and height of the beam profile by cylindrical lenses and ensuring a similar beam path inside the crystals. The location of the isolator between the amplifier stages ensures a high overall efficiency

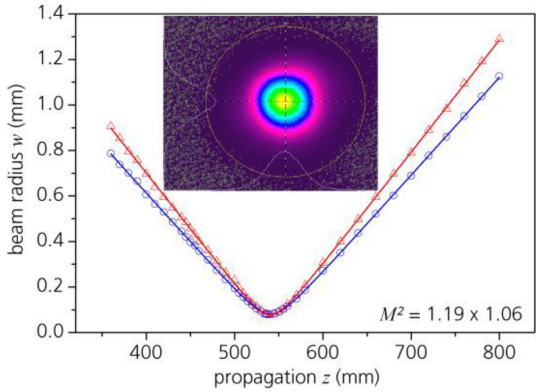

Fig. 21. Beam radius at $P = 530$ W output power of system in Fig. 20 with spatially filtering and typical beam profile (inset).

and effective protection of the system due to the low gain of the last stage. The loss of 7% power in Fig. 17 is made up of about 3% loss at the isolator, 2% depolarization of the first stage and 2% at seven lenses of the imaging optics.

The seeder is a commercial fiber-laser system (Menlo Systems) adapted to the center wavelength and bandwidth of Yb:YAG, an adjustable repetition rate of 10–100 MHz and the option to stabilize repetition rate and carrier-envelope offset frequency. For maximum efficiency, good beam quality and low ASE, the output is further amplified and spatially filtered in an end-pumped double-pass Yb:YAG rod type amplifier. Innoslab amplifiers are sensitive to pointing of the seed source of more than 10% in the beam divergence. Therefore, an active stabilization of the beam pointing (TEM Messtechnik) is located directly in front of the first Innoslab amplifier. This is necessary due to thermal issues of the fiber and most other commercial laser front ends, most notably systems incorporating a CPA.

3) Spatial Filtering: The beam quality of $M^2 \sim 1.4$ in slow-axis is a representative value for an Innoslab MOPA system as seen in Fig. 17. The characteristic *sinc*-like diffraction patterns in the far-field cannot be suppressed by alignment only (Section III-C). They arise by cropping a small amount at the margins of the out-coupled light *field,* resulting in a pronounced modulation of the light *intensity* in the far-field, although the overlap with a fundamental mode remains very high. The diffraction patterns can be quite disruptive for precise micromachining or by heating optics in the application beam path. By spatial filtering in the slow-axis far-field of the Innoslab amplifier, the diffraction pattern can be removed and beam quality improved with only small power loss.

A typical setup of such a system is depicted in Fig. 20. The MOPA is the same as in Fig. 17, but the repetition rate is decreased to 10 MHz and the average output power to 580 W at the same time to limit the B-integral to a safe level. The spatial filter is realized as a high-reflective mirror with a 320 μm slit in the focal plane of a cylindrical lens of 500 mm focal length behind the second Innoslab amplifier stage (Fig. 22).

By clipping 9% of the power, the beam quality is improved in the slow-axis from $M^2 = 1.35$ to 1.17. The beam profile is smooth and diffraction patterns are absent in the filtered beam

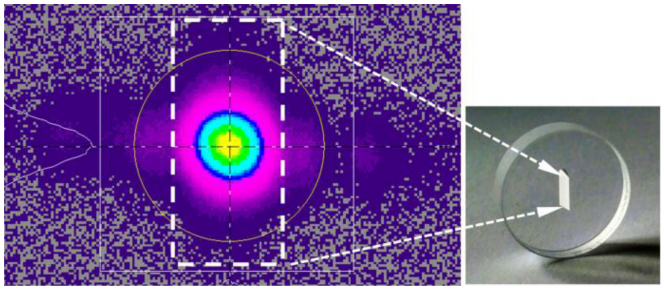

Fig. 22. Beam profile in far-field of Innoslab amplifier (left) and slit-like aperture in HR-mirror, produced by Inverse Laser Drilling (right).

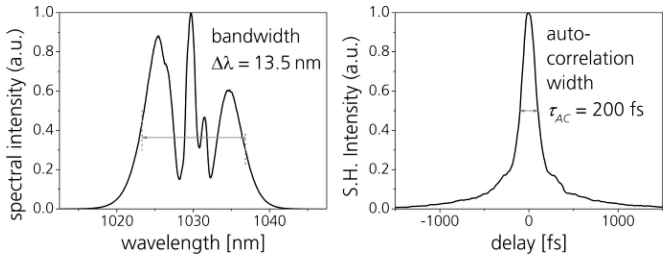

Fig. 23. Measured spectrum (left) and autocorrelation (right) at $P = 375$ W and $E = 37.5$ μJ.

(Fig. 21). Since the spatial filter is implemented by a slit in a dielectric mirror, it can be easily aligned and the aperture withstands the full average power, no matter if the beam hits the middle, edge or outside the slit.

The slit mirror is manufactured by Inverse Laser Drilling. In this patented process [63], the uncoated mirror substrate is placed on a vertically movable translation table with the mirror surface facing upwards. The laser beam is focused through the top surface onto the bottom surface of the bulk. The beam is deflected by scanning mirrors in the horizontal plane; this way the slit geometry's bottom layer is ablated. By moving the translation table and ablating layers step by step the entire slit geometry can be ablated or "drilled". To take the beam divergence into account, the slit is undercut with an angle of 8° [64].

4) Pulse Compression: For some applications such as high harmonic generation [65] or material processing [66] shorter pulse durations than those supported by Yb:YAG are worthwhile. Basically active media other than Yb:YAG can be used to achieve shorter pulse durations. Such a material ideally combines the excellent thermo-optical properties for high average power and large emission cross section for high gain of Yb:YAG with a broad amplification bandwidth. Unfortunately, the product of emission cross section, lifetime of the upper state and bandwidth is roughly invariant. The penalty for higher bandwidth is lower gain, thereby a higher number of passes or lower efficiency of the Innoslab amplifier. This can be tolerated to some extent; Yb:Lu_2O_3 is a promising material, which has a 1.5 times broader emission bandwidth than Yb:YAG [67], but similar thermo-optical properties. Pulses <500 fs are feasible, but pulse durations <200 fs cannot be addressed by Innoslab amplifiers directly and requires an OPCPA or nonlinear pulse compression unit.

The nonlinear pulse compression consists of a nonlinear medium for spectral broadening by self-phase modulation and a dispersive compressor to compensate the resulting chirp. Most common is a fused silica fiber for the nonlinear medium. But damage of the fiber by catastrophic self-focusing limits the pulse peak power to $P_{\mathrm{crit}} \approx 6$ MW. This corresponds to a pulse energy of $E \approx 5$ μJ for pulses with $\tau_p = 850$ fs. Pulses with 680 fs and $\sim$2 μJ at 20.8 MHz repetition rate of a 1-stage amplifier system are spectrally broadened to a spectral width of $\Delta\lambda \approx 80$ nm in a LMA fiber of 7.1 cm length [67]. The pulses are compressed with chirped mirrors with an accumulated GDD of -6000 fs^2 to $\tau_p = 35$ fs. The transmission of the complete compression unit is about 60%, leading to a pulse energy $E \approx 1.2$ μJ. For pulse compression with higher pulse energies, a nonlinear medium with a higher critical power is required. Gas-filled hollow-core fibers can be used for energies above $\sim$200 μJ [68].

For pulses with an energy of 5 μJ $< E <$ 200 μJ a new compression scheme was demonstrated using the 2-stage Yb:Innoslab amplifier system [69]. Here the spectral broadening is split up into 38 passes, each having a beam diameter of $w \approx 1.1$ mm inside 20 mm of fused silica. Between the passes in fused silica, the beam propagates in air, hence critical self-focusing is prevented [69]. A chirped mirror compressor is used to compensate the chirp. With the Innoslab amplifier system described above, the pulse duration is compressed from $\tau_p = 830$ fs to $\tau_p < 170$ fs at a spectral bandwidth $\Delta\lambda \approx 13$ nm (Fig. 23). Pulses with a pulse energy $E = 37.5$ μJ are achieved at an average power of $P = 375$ W and a beam quality factor of $M^2 = 1.38 \times 1.33$ behind the nonlinear compression. The transmission of the compression unit is 91%.

VIII. Conclusion

Innoslab amplifiers find various applications in industry and science. Parameters range from single-frequency operation to ultrafast pulses.

They hold their ground in a competitive environment of other laser concepts having great strengths but weaknesses as well, because of their well-balanced properties in the 10–1000 W output power range. Their very good thermal management and the single-pass amplification, comprising beam expansion during multiple passes through the crystal stands out in particular. Innoslab amplifiers match the emission characteristics of high power diode lasers, thereby permitting high pump intensity, gain and efficiency. Short beam propagation distances in the laser crystal keep self phase modulation, stimulated Brillouin scattering, Raman scattering and dispersion low.

Innoslab amplifiers are advantageous wherever good beam quality, spectral properties, efficiency or a compact setup are essential. Innoslabs typically amplify cw radiation, pulses at arbitrary repetition rates and pulse trains of fs to ns pulse duration by a factor of 10–1000 up to some 10 mJ pulse energy and 100–1000 W output power. Pulse energy up to the Joule level at amplification factors of 10–100 and 10–100 W average power are addressed by pulsed pumped Innoslab amplifiers. The

concept can be adapted to a broad range of laser materials, including exotic ones.

Innoslab amplifiers are technically mature, but still not fully exploited. Novel amplifier resonators offer a gain of up to 10^5 in one amplification stage. The increase in brightness of diode lasers enables a new generation of simplified and even more compact amplifiers. Up to 5 kW average power, a few Joule pulse energy or 100 GW peak power are conceivable, if demanded by applications and the market.

REFERENCES

[1] K. Du, "Optically pumped intensifying agent, in particular a solid state agent," U.S. Patent 6 351 477 B1, Feb. 26, 2002.

[2] K. Du, P. Loosen, and R. Poprawe, "Optical amplifier arrangement for a solid state laser," U.S. Patent 6 654 163 B1, Nov. 25, 2003.

[3] C. Schnitzler, M. Hofer, J. Luttmann, D. Hoffmann, and R. Poprawe, "A cw kW-class diode end pumped Nd:YAG slab laser," in *Proc. Tech. Dig. CLEO*, 2002, pp. 766–768.

[4] J. Luttmann, K. Nicklaus, V. Morasch, S. Fu, M. Höfer, M. Traub, D. Hoffmann, R. Treichel, C. Wührer, and P. Zeller, "Very high-efficiency frequency-tripled Nd:YAG MOPA for space-borne LIDAR," *Proc. SPIE*, vol. 6871, pp. 687109-1–687109-12, 2008.

[5] T. Brand and F. Hollinger, "Diode-pumped slab and rod lasers with high cw output power," in *Laser in Research and Engineering*. Berlin, Germany: Springer, 1996, pp. 367–370.

[6] A. K. Sridharan, S. Saraf, S. Sinha, and R. L. Byer, "Zigzag slabs for solid-state laser amplifiers: Batch fabrication and parasitic oscillation suppression," *Appl. Opt.*, vol. 45, pp. 3340–3351, May, 2006.

[7] W. Koechner, *Solid-State Laser Engineering*, 6th ed. New York, NY, USA: Springer Science + Business Media, 2006.

[8] D. P. Shepherd, S. J. Hettrick, C. Li, J. I. Mackenzie1, R. J. Beach, S. C. Mitchell, and H. E. Meissner, "High-power planar dielectric waveguide Lasers," *Appl. Phys. D*, vol. 34, pp. 2420–2432, Aug. 2001.

[9] J. R. Lee, H. J. Baker, G. J. Friel, G. J. Hilton, and D. R. Hall, "High-average-power Nd:YAG planar waveguide laser that is face pumped by 10 laser diode bars," *Opt. Lett.*, vol. 27, no. 7, pp. 524–526, Apr. 2002.

[10] N. Hodgson and H. Hoffman, "Diode-pumped slab solid-state laser," U.S. Patent 20 020 181 534 A1, Dec. 25, 2002.

[11] A. Dergachev, J. H. Flint, Y. Isyanova, B. Pati, E. V. Slobodtchikov, K. F. Wall, and P. F. Moulton, "Review of multipass slab laser systems," *IEEE J. Sel. Topics Quantum Electron.*, vol. 13, no. 3, pp. 647–660, May 2007.

[12] S. P. Chard and M. J. Damzen, "Compact architecture for power scaling bounce geometry lasers," *Opt. Exp.*, vol. 17, no. 4, pp. 2218–2220, Feb. 2009.

[13] T. Mans, P. Russbueldt, J. Weitenberg, G. Rotarius, D. Hoffmann, and R. Poprawe, "Yb:KYW Innoslab-Amplifier," in *Proc. Conf. Lasers, Electro-Opt./Eur. Quantum Electron. Conf.*, Jun. 2009, p. 1.

[14] S. Chénais, F. Balembois, F. Druon, G. Lucas-Leclin, and P. Georges, "Thermal lensing in diode-pumped ytterbium lasers—part I: Theoretical analysis and wavefront measurements," *IEEE J. Quantum Electron.*, vol. 40, no. 9, pp. 1217–1234, Sep. 2004.

[15] M. Traub, H.-D. Hoffmann, H.-D. Plum, K. Wieching, P. Loosen, and R. Poprawe, "Homogenization of high power diode laser beams for pumping and direct applications," *Proc. SPIE*, vol. 6104, pp. 6104Q-1–6104Q-10, 2006.

[16] P. Loosen and A. Knitsch, "Incoherent beam superposition," in *High Power Diode Lasers and Applications*, 1st ed., F. Bachmann, P. Loosen, and R. Poprawe, Eds. New York, NY, USA: Springer Science + Business, 2010, pp. 139–142.

[17] A. G. Fox and T. Li, "Resonant modes in an optical maser," in *Proc. IRE(Correspondence)*, vol. 48, pp. 1904–1905, 1960.

[18] T. J. Kane and R. L. Byer, "Monolithic, unidirectional single-mode Nd:YAG ring laser," *Opt. Lett.*, vol. 10, no. 2, pp. 65–67, Feb. 1985.

[19] I. Freitag, A. Tunnermann, and H. Welling, "Power scaling of diode-pumped monolithic Nd:YAG lasers to output powers of several watts," *Opt. Commun.*, vol. 115, no.5–6, pp. 511–515, Apr. 1995.

[20] M. Höfer, M. Traub, R. Kleindienst, H. Sipma, H.-D. Hoffmann, P. Wessels, and P. Burdack, "Multi ten watt, ultra-stable and tuneable innoslab based single frequency MOPA," *Proc. SPIE*, vol. 6451, pp. 1–7, 2007.

[21] M. Wirth, A. Fix, P. Mahnke, H. Schwarzer, F. Schrandt, and G. Ehret, "The airborne multi-wavelength water vapor differential absorption lidar WALES: System design and performance," *Appl. Phys. B*, vol. 96, pp. 201–213, Jul. 2009.

[22] J. Löhring, J. Luttmann, R. Kasemann, M. Schlösser, J. Klein, D. Hoffmann, A. Amediek, C. Büdenbender, A. Fix, M. Wirth, M. Quatrevalet, and G. Ehret, "INNOSLAB-based single-frequency MOPA for airborne LIDAR detection of CO_2 and methane," *Proc. SPIE*, vol. 8959, pp. 89590J–1–89590J-8, 2014.

[23] J. Löhring, M. Schlösser, and D. Hoffmann, "Compositionally tuned Nd:(YxLu1-x)3Ga5O12-laser at 935 nm for H_2O-dial systems," *Proc. SPIE*, vol. 7912, pp. 79121N-1–79121N-10, 2011.

[24] J. Löhring, "Laserstrahlquellen auf basis eines neuartigen neodym-dotierten mischgranats für wasserdampf-DIAL-systeme bei 935 nm," Ph.D. dissertation, Dept. Mech. Eng., RWTH, Aachen, Germany, 2011.

[25] J. Löhring, K. Nicklaus, N. Kujath, and D. Hoffmann, "Diode pumped Nd:YGG laser for direct generation of pulsed 935 nm radiation for water vapour measurements," *Proc. SPIE*, vol. 6451, pp. 64510I–1-64510I-8, 2007.

[26] J. Löhring, A. Meissner, V. Morasch, P. Becker, W. Heddrich, and D. Hoffmann, "Single-frequency Nd:YGG laser at 935 nm for future water-vapour DIAL systems," *Proc. SPIE*, vol. 7193, pp. 71931Y-1–71931Y-7, 2009.

[27] J. Löhring, A. Meissner, D. Hoffmann, A. Fix, G. Ehret, and M. Alpers, "Diode-pumped single-frequency-Nd:YGG-MOPA for water–vapor DIAL measurements: Design, setup and performance," *Appl. Phys. B*, vol. 102, pp. 917–935, Mar. 2011.

[28] A. Fix, G. Ehret, J. Löhring, D. Hoffmann, and M. Alpers, "Water vapor differential absorption LIDAR measurements using a diode-pumped all-solid-state laser at 935 nm," *Appl. Phys. B*, vol. 102, pp. 905–915, Mar. 2011.

[29] Z. Ma, D.-J. Li, P.-X. Hu, A. Schell, P. Shi, C.-R. Haas, N.-L. Wu, and K.-M. Du, "Monolithic Nd:YVO4 slab oscillator-amplifier," *Opt. Lett.*, vol. 32, pp. 1262–1264, Apr. 2007.

[30] Z. Ma, D.-J. Li, P. Shi, P.-X Hu, N.-L. Wu, and K.-M. Du, "Compact multipass Nd:YVO4 slab laser amplifier," *J. Opt. Soc. B*, vol. 24, pp. 1061–1065, Apr. 2007.

[31] J. Löhring, M. Höfer, R. Wester, D. Hoffmann, and R. Poprawe, "Thermal effects on the scalability of high power third harmonic generation at 355 nm in LBO," presented at the Proc. Adv. Solid-State Photon., Incline Village, NV, USA, 2006, Paper TuB24.

[32] A. Meissner, P. Kucirek, J. Li, S. Yang, M. Hoefer, and D. Hoffmann, "Simulations and experiments on resonantly-pumped single-frequency Erbium lasers at 1.6 μm," *Proc. SPIE*, vol. 8599, pp. 85990H-1–85990H-8, 2013.

[33] A. Meissner, P. Kucirek, and H.-D. Hoffmann, "Resonantly-pumped single-frequency Er:YLuAG-laser with pulsed emission at 1645.2 nm (air)," presented at the 5th EPS-QEOD EUROPHOTON Conf., Stockholm, Sweden, Aug. 26–31, 2012.

[34] U. N. Singh, J. Yu, Y. Bai, M. Petros, and R. T. Menzies, "Development of a pulsed 2-micron laser transmitter for CO_2 sensing from space," presented at NASA Earth Sci. Technol. Forum, Pasadena, CA, USA, 2011. [Online]. Available: http://esto.nasa.gov/conferences/estf2011/presentations/Singh_ESTF2011.pdf

[35] M. Eichhorn, "Quasi-three-level solid-state lasers in the near and mid infrared based on trivalent rare earth ions," *Appl. Phys. B*, vol. 93, pp. 269–319, Sep. 2008.

[36] J. W. Kim, J. I. Machenzie, and W. A. Clarkson, "Influence of energy-transfer-upconversion on threshold pump power in quasi-three-level solid-state lasers," *Opt. Exp.*, vol. 17, no. 14, pp. 11935–11943, Jul. 2009.

[37] H. J. Strauss, W. Koen, C. Bollig, M. J. D. Esser, C. Jacobs, O. J. P. Collet, and D. R. Preussler, "Ho:YLF & Ho:LuLF slab amplifier system delivering 200 mJ, 2 μm single-frequency pulses," *Opt. Exp.*, vol. 19, no. 15, pp. 13974–13979, Jul. 2011.

[38] J. Li, S. H. Yang, A. Meissner, M. Höfer, and H. D. Hoffmann, "A 200 W INNOSLAB Tm:YLF Laser," *Laser Phys. Lett.*, vol. 10, no. 5, pp. 055002-1–055002-5, Mar. 2013.

[39] A. Nebel, T. Herrmann, B. Henrich, R. Knappe, "Generation of tailored picosecond-pulse-trains for micro-machining," *Proc. SPIE*, vol. 6108, pp. 610812-1–610812-8, 2006.

[40] B. Luther-Davies, V. Z. Kolev, M. J. Lederer, N. R. Madsen, A. V. Rode, J. Giesekus, and M. Duering, "Table-top 50-W laser system for ultra-fast laser ablation," *Appl. Phys. A*, vol. 79, no. 4–6, pp. 1051–1055, 2004.

[41] D. Li and K. Du, "Picosecond laser with 400 W average power and 1mJ pulse energy," *Proc. SPIE*, vol. 7912, p. 79120N, 2011.
[42] C. Heese, A. E. Oehler, L. Gallmann, and U. Keller, "High-energy picosecond Nd: YVO4 slab amplifier for OPCPA pumping," *Appl. Phys. B*, vol. 103, no. 1, pp. 5–8, Apr. 2011.
[43] L. Xu, H. Zhang, Y. Mao, Y. Yan, Z. Fan, and J. Xin, "High-average-power and high-beam-quality Innoslab picosecond laser amplifier," *Appl. Opt.*, vol. 51, no. 27, pp. 6669–6672, Sep. 2012.
[44] H. Lin, J. Li, and X. Liang, "105 W,$<$10 ps, TEM 00 laser output based on an in-band pumped Nd: YVO_4 Innoslab amplifier," *Opt. Lett.*, vol. 37, no. 13, pp. 2634–2636, Jun. 2012.
[45] C. Tulea, J. Caron, H. Wahab, N. Gehlich, M. Hoefer, D. Esser, and R. Noll, "Highly efficient nonthermal ablation of bone under bulk water with a frequency-doubled Nd: YVO4 picosecond laser," *Proc. SPIE*, vol. 8565, p. 85656E, 2013.
[46] D. Esser, D. Hoffmann, B. Jungbluth, and R. Poprawe, "Regenerative amplification of laser diode pulses with variable pulse duration from ps to ns range," in *Proc. CLEO/Eur.*, 2003, p. 34.
[47] P. Loosen, M. Höfer, D. Esser, H. Sipma, R. Kasemann, and H. D. Hoffmann, "Advanced INNOSLAB solid-state-lasers for the generation of bright XUV/EUV-radiation," presented at Int. Workshop Extreme Ultraviolet Sources, Dublin, Ireland, Nov. 13–15, 2010. [Online]. Available: http:/www.euvlitho.com/2010/P37.pdf
[48] H. Legall, G. Blobel, H. Stiel, W. Sandner, C. Seim, P. Takman, D. Martz, M. Selin, U. Vogt, H. Hertz, D. Esser, H. Sipma, J. Luttmann, M. Höfer, H.-D. Hoffmann, S. Yulin, T. Feigl, S. Rehbein, P. Guttmann, G. Schneider, U. Wiesemann, M. Wirtz, and W. Diete, "Compact x-ray microscope for the water window based on a high brightness laser plasma source," *Opt. Exp.*, vol. 20, no. 16, pp. 18362–18369, Jul. 2012.
[49] D. Martz, M. Selin, O. von Hofsten, E. Fogelqvist, A. Holmberg, U. Vogt, H. Legall, G. Blobel, C. Seim, H. Stiel, and H. Hertz, "High average brightness water window source for short-exposure ps cryomicroscopy," *Opt. Lett.*, vol. 37, no. 21, pp. 4425–4427, Nov. 2012.
[50] H. Legall, H. Stiel, G. Blobel, C. Seim, J. Baumann, S. Yulin, D. Esser, M. Hoefer, U. Wiesemann, M. Wirtz, and H. M. Hertz, "A compact laboratory transmission X-ray microscope for the water window," *J. Phys.: Conf. Ser.*, vol. 463, pp. 012013-1–012013-4, Oct. 2013.
[51] P. H. Russbueldt, T. Mans, D. H. Hoffmann, and R. Poprawe, "High power Yb:YAG Innoslab Fs-amplifier," presented at Conf. Lasers Electro-Opt., OSA Tech. Digest, San Jose, CA, USA, 2008, Paper CTuK5.
[52] P. Russbueldt, T. Mans, G. Rotarius, J. Weitenberg, H. D. Hoffmann, and R. Poprawe, "400 W Yb:YAG Innoslab fs-amplifier," *Opt. Exp.*, vol. 17, pp. 12230–12245, Jul. 2009.
[53] P. H. Russbueldt, T. Mans, G. Rotarius, D. Hoffmann, R. Poprawe, T. Eidam, J. Limpert, and A. Tünnermann, "Hybrid 400 W fiber-innoslab fs-amplifier," presented at the Adv. Solid-State Photon., OSA Tech. Digest Series (CD), Denver, CO, USA, 2009, Paper MF4.
[54] P. Russbueldt, T. Mans, J. Weitenberg, H. D. Hoffmann, and R. Poprawe, "Compact diode-pumped 1.1 kW Yb:YAG Innoslab femtosecond amplifier," *Opt. Lett.*, vol. 35, pp. 4169–4171, Dec. 2010.
[55] T. Mans, Jan Dolkemeyer, P. Russbüldt, and C. Schnitzler, "Highly flexible ultrafast laser system with 260 W average power," *Proc. SPIE*, vol. 7912, pp. 79120M-1–79120M-6, Feb. 2011.
[56] T. Mans, C. Hönninger, J. Dolkemeyer, A. Letan, C. Schnitzler, and E. Mottay, "200 W fs Innoslab amplifier with 400 μJ pulse energy for industrial applications," *Proc. SPIE*, vol. 8599, pp. 859915-1–859915-4, 2013.
[57] M. Schulz, R. Riedel, A. Willner, T. Mans, C. Schnitzler, P. Russbueldt, J. Dolkemeyer, E. Seise, T. Gottschall, S. Hädrich, S. Duesterer, H. Schlarb, J. Feldhaus, J. Limpert, B. Faatz, A. Tünnermann, J. Rossbach, M. Drescher, and F. Tavella, "Yb:YAG Innoslab amplifier: Efficient high repetition rate subpicosecond pumping system for optical parametric chirped pulse amplification," *Opt. Lett.*, vol. 36, no. 13, pp. 2456–2458, Jul. 2011.
[58] T. Mans, R. Graf, J. Dolkemeyer, and C. Schnitzler, "Femtosecond Innoslab amplifier with 300 W average power and pulse energies in the mJ-regime," *Proc. SPIE*, vol. 8959, pp. 895916-1–895916-4, 2014.
[59] R. Riedel, A. Stephanides, M. J. Prandolini, B. Gronloh, B. Jungbluth, T. Mans, and F. Tavella, "Power scaling of supercontinuum seeded megahertz-repetition rate optical parametric chirped pulse amplifiers," *Opt. Lett.*, vol. 39, pp. 1422–1424, Mar. 2014.
[60] A. Vernaleken, J. Weitenberg, T. Sartorius, P. Russbueldt, W. Schneider, S. L. Stebbings, M. F. Kling, P. Hommelhoff, H.-D. Hoffmann,– R. Poprawe, F. Krausz, T. W. Hänsch, and T. Udem, "Single pass high harmonic generation at 20.8 MHz repetition rate," *Opt. Lett.*, vol. 36, no. 17, pp. 3428–3430, Sep. 2011.
[61] S. Chénais, F. Balembois, F. Druon, G. Lucas-Leclin, and P. Georges, "Thermal lensing in diode-pumped ytterbium lasers—part II: Evaluation of quantum efficiencies," *IEEE J. Quantum Electron.*, vol. 40, no. 9, pp. 1235–1243, Sep. 2004.
[62] P. Russbueldt, J. Weitenberg, T. Sartorius, G. Rotarius, H. D. Hoffmann, and R. Poprawe, "Ytterbium Innoslab amplifiers—The high average power approach of ultrafast lasers," in *Proc. AIP Conf. Proc.*, 2012, vol. 1462, pp. 120–124.
[63] K. Du, P. Loosen, and R. Poprawe, "Verfahren für die Materialbearbeitung und Verwendung desselben," German Patent DE10 029110 B4, May 18, 2006.
[64] D. Esser, W. Bröring, J. Weitenberg, and H.-D. Hoffmann, "Laser-manufactured mirrors for geometrical output coupling of intracavity-generated high harmonics," *Opt. Exp.*, vol. 21, no. 22, pp. 26797–26805, Oct. 2013.
[65] A. L'Huillier, K. J. Schafer, and K. C. Kulander, "Theoretical aspects of intense field harmonic generation," *J. Phys. B.*, vol. 24, no. 15, pp. 3315–3341, Aug. 1991.
[66] X. Liu, D. Du, and G. Mourou, "Laser ablation and micromachining with ultrashort laser pulses," *IEEE J. Quantum Electron.*, vol. 33, no. 10, pp. 1706–1716, Oct. 1997.
[67] R. Peters, C. Kränkel, K. Petermann, and G. Huber, "Broadly tunable high-power Yb:Lu_2O_3 thin disk laser with 80% slope efficiency," *Opt. Exp.*, vol. 15, no. 11, pp. 7075–7082, May 2007.
[68] J. Rothhardt, S. Hädrich, H. Carstens, N. Herrick, S. Demmler, J. Limpert, and A. Tünnermann, "1 MHz repetition rate hollow fiber pulse compression to sub-100-fs duration at 100 W average power," *Opt. Lett.*, vol. 36, no. 23, pp. 4605–4607, Dec. 2011.
[69] T. Sartorius, J. Schulte, J. Weitenberg, and P. Russbueldt, "Nonlinear compression in a multi-pass cell," unpublished paper.

Peter Russbueldt was born in Jülich, Germany, in 1970. He received the Ph.D. degree in physics from RWTH Aachen University, Aachen, Germany, in 2004.

Since 1995, he has been working at the Chair for Laser Technology (LLT) of RWTH Aachen University and at the Fraunhofer Institute for Laser Technology (ILT), Aachen. Currently, he is managing the group "Ultrafast Lasers" at ILT. His main research interests include development of femtosecond oscillators and amplifiers based on various laser materials, involving its metrology and application.

He is a Member of the Optical Society of America. He was a recipient of the Borchers badge (RWTH Aachen University), Stifterverband Science Prize (Stifterverband für die Deutsche Wissenschaft), and Berthold Leibinger Innovationspreis (second price, Berthold Leibinger Stiftung).

Dieter Hoffmann was born in Gerolstein, Germany, in 1961. He received a degree in electrical engineering from the FH Aachen University of Applied Sciences in 1988 and a degree in communications engineering from RWTH Aachen University, Aachen, Germany, in 1992.

From 1993 to 1996, he was a Research Assistant at the Chair for Laser Technology (LLT) of the RWTH Aachen University. From 1997 to 2001, he was a Research Assistant at the Fraunhofer Institute for Laser Technology (Fraunhofer ILT), Aachen. From 2001 to 2010, he was the Head of the Department for Lasers and Laser Optics, Fraunhofer ILT, and since 2010, he has been a Competence Area Manager, responsible for six working groups covering the Fraunhofer ILT activities in the field of lasers and laser optics. His research interests include high-power lasers and optics for applications in industry and science. He holds several patents.

Mr. Hoffmann received the Fraunhofer Award in 1999 for the development of the first industrial diode.pumped multi-kW solid-state laser, the Berthold Leibinger Innovationspreis (second price, Berthold Leibinger Stiftung) in 2012 for his contribution to the Innoslab Laser Development and the Stifterverband Science Prize for his contribution on laser sources for "Ultra-short laser pulses for science and industry."

Marco Höfer was born in Bendorf, Germany, in 1975. He received a diploma degree in physics from the RWTH Aachen University, Aachen, Germany.

Since 2001, he has been working at the Fraunhofer Institute for Laser Technology (ILT), Aachen. He currently manages the group "Solid State Lasers" at ILT. During this time, he has been working on different research topics including Innoslab oscillators and amplifiers, nonlinear optics, and simulation tools for wave optics and nonlinear optics.

As a member in different teams, Mr. Höfer received the national Stifterverband Science Prize (Stifterverband für die Deutsche Wissenschaft), the International Innovation Award Laser Technology (European Laser Institute), and the Berthold Leibinger Innovationspreis (second price, Berthold Leibinger Stiftung).

Jens Löhring was born in Stadtlohn, Germany, in 1977. He studied physics at RWTH Aachen University, Aachen, Germany, and Universitá degli Studi di Trieste, Trieste, Italy, and received the Ph.D. degree in physics from RWTH Aachen University, in 2012.

Since 2004, he has been working at the Fraunhofer Institute for Laser Technology, Aachen. Currently, he is mainly working on the development of pulsed single-frequency laser sources for airborne and spaceborne LIDAR applications.

Dr. Löhring was the recipient of the Best Student Paper Award (Coherent), the Schöneborn prize and Borchers badge (RWTH Aachen University), and the Berthold Leibinger Innovationspreis (second price, Berthold Leibinger Stiftung).

Jörg Luttmann studied physics at RWTH Aachen University, Aachen, Germany, and received the Diploma degree in 2002.

Since 2001, he has been working at the Fraunhofer Institute for Laser Technology, Aachen. His current research interests include development of solid-state lasers, especially for airborne and spaceborne applications.

Ansgar Meissner was born in Gelsenkirchen, Germany, in 1981. He received the Diploma degree in physics from the RWTH Aachen University, Aachen, Germany, and the University of Edinburgh, Edinburgh, U.K., in 2008.

Since 2007, he has been working at the Fraunhofer Institute for Laser Technology, Aachen, with the Solid-State-Lasers group. His research interests include laser beam sources in the IR-B band with Erbium-, Thulium-, and Holmium-doped gain media, pulsed single-frequency lasers, and laser-induced damage testing of optical components.

Johannes Weitenberg was born in Rhede, Germany, in 1981. He studied physics at RWTH Aachen University, Aachen, Germany, and received the Diploma degree in 2007.

Since 2008, he has been working at the Chair for Laser Technology of RWTH Aachen University and at the Fraunhofer Institute for Laser Technology, Aachen. His current research interests include development of solid-state lasers, high harmonic generation, enhancement resonators, and nonlinear pulse compression.

Mr. Weitenberg is a member of Deutsche Physikalische Gesellschaft and the Optical Society of America. He was a recipient of the Stifterverband Science Prize (Stifterverband für die Deutsche Wissenschaft) and Berthold Leibinger Innovationspreis (second price, Berthold Leibinger Stiftung).

Martin Traub studied mechanical engineering at RWTH Aachen University, Aachen, Germany, and Michigan State University, East Lansing, MI, USA, and industrial engineering at RWTH Aachen University.

Since 1999, he has been working at the Fraunhofer Institute for Laser Technology (ILT), Aachen. Currently, he is managing the group "Optics Design and Diode Lasers." His research interests include beam shaping and fiber coupling of high-power diode lasers as well as imaging and nonimaging optics.

Mr. Traub is a member of the Deutsche Gesellschaft für angewandte Optik (DGaO). He was a recipient of the Springorum Prize (RWTH Aachen University) and the Stifterverband Science Prize (Stifterverband für die Deutsche Wissenschaft).

Thomas Sartorius was born in Köln, Germany, in 1984. He studied physics at RWTH Aachen University, Aachen, Germany, and received the Diploma degree in 2011.

Since 2007, he has been working at the Fraunhofer Institute for Laser Technology, Aachen. His current research interests include development of high-power ultrafast amplifiers and nonlinear pulse compression.

Mr. Sartorius is a Member of the Deutsche Physikalische Gesellschaft.

Dominik Esser received the Diploma degree in physics from RWTH Aachen University, Aachen, Germany, and the Diploma degree in economics from Fernuniversität Hagen, Hagen, Germany.

Since 2001, he has been working at the Fraunhofer Institute for Laser Technology, Aachen. His current research interests include development of solid-state lasers and laser drilling of dielectric materials.

Mr. Esser is a Member of the Deutsche Physikalische Gesellschaft and the Optical Society of America.

Rolf Wester was born in Frankfurt, Germany, in 1956. He received the M.S. degree in physics from the Technical University Darmstadt, Darmstadt, Germany, in 1981, and the Ph.D. degree from RWTH Aachen University, Aachen, Germany, in 1985.

Since 1987, he has been a Scientist with the Fraunhofer Institute for Laser Technology, Aachen, where he was involved in the development of RF and GHz discharges for the excitation of CO_2, excimer and argon lasers and in the development of diode-pumped Nd:YAG lasers. His research interests include modeling of optical wave fields, e.g., in laser resonators, nonlinear optics, freeform optical design, and development of software for the data analysis and control of laser-based measuring systems.

Dr. Wester is a Member of the Optical Society of America.

Peter Loosen was born in Wittlich, Germany, in 1955. He received the Ph.D. degree in physics from the TU Darmstadt, Darmstadt, Germany, in 1984.

From 1985 to 1993, he was the Head of the department "Gas Lasers." Since 1989, he has been in charge of the departments "Solid-State Lasers," "Metrology," and "Plasma Systems," and since 1993, he has been the Deputy Head of the Fraunhofer Institute for Laser Technology, Aachen, Germany. In 2004, he was appointed a Professor for "Technology of Optical Systems" and head of the newly formed respective institute at RWTH Aachen University, Aachen. He is editor of and contributor in four books and author or coauthor of more than 140 papers and more than 40 inventions. His research interests include fundamentals and the technology of lasers and laser systems for industrial manufacturing, industrial high-power gas-, solid-state and diode lasers, integration of such lasers into production applications and optical systems for laser and laser systems.

Dr. Loosen is a Member of several editorial boards and head of organizational committees in the field of laser and laser applications, for instance for IEEE committees and publications. He is General Chair of the "World of Photonics Congress" Munich, 2009–2015. His awards and honors include the Fraunofer Price (Fraunhofer association) and Berthold Leibinger Innovationspreis (second price, Berthold Leibinger Stiftung).

Reinhart Poprawe was born in Offenbach/Main, Germany, in 1954. He studied physics at the University of Mainz, Mainz, Germany; California State University, Los Angeles, CA, USA; and TU Darmstadt, Darmstadt, Germany, and graduated in physics from the TU Darmstadt, in 1979.

From 1980 to 1985, he was a Scientific Assistant at the TU Darmstadt, from 1985 to 1989 the Head of the department at the Fraunhofer Institute for Laser Technology (ILT), Aachen, Germany, and from 1989 to 1996 the CEO of Thyssen Laser-Technology GmbH, Aachen. Since 1996, he has been a Professor of Laser Technology at RWTH Aachen University and the Head of the Fraunhofer ILT. From 2005 to 2008, he was the Vice-Rector for Structure, Research, and Young Academics of RWTH Aachen University and since 2008 Rector's Delegate for China. He is the editor of and contributor in five books and author or coauthor of more than 300 papers and holds more than 15 patents. His current and previous research interests include laser applications like drilling, cutting, joining (welding, soldering), surface treatment, laser additive manufacturing, rapid manufacturing, polishing, microtechnology, system technology, process control, photonics in life science, and direct photonic production. In laser development, he focuses on diode-pumped solid-state lasers, diode lasers, pump modules, and amplifiers for multisectorial applications (information and communication technology, display, EUV-lithography, ps and fs lasers), coherent coupling, incoherent superposition, beam shaping in space and time, ultrafast lasers, and production processes for diode lasers.

Dr. Poprawe is a Member of the Arbeitskreis Lasertechnik e.V. Aachen, the wissenschaftlichen Gesellschaft Lasertechnik WLT e.V., the North Rhine-Westphalia Academy of Sciences. He is a Fellow of the Society of Manufacturing Engineers and the Laser Institute of Amerika (LIA). He is a Board Member of the LIA, the National Laser Centre of South Africa, the Coopération Laser Franco-Allemande, and several other institutions. He has spun off approximately 30 companies; he holds shares in several of them. His awards and honors include the Fraunhofer Prize (1987), the Innovation Prize of North Rhine-Westphalia (2011), and an Honorary Professorship from Tsinghua University, Beijing (2014).